MICHIGAN STATE UNIVERSITY

CYCLOTRON LABORATORY

HEAVY ION DYNAMICS FROM THE POINT OF VIEW OF CLASSICAL MEAN FIELD THEORY

ALDO BONASERA

TO BE PUBLISHED IN NUCLEAR PHYSICS A

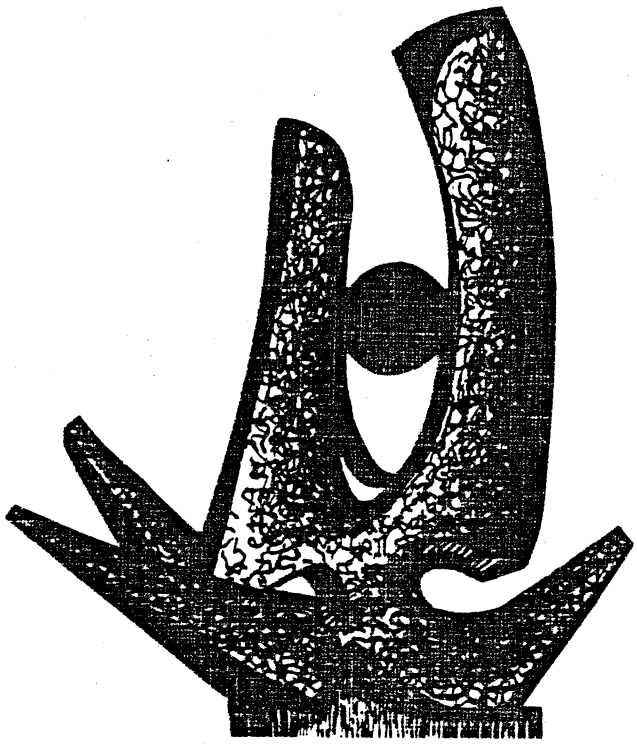

FEBRUARY 1985

MSUCL-485

MSU-CL 485
February 1985

Heavy Ion Dynamics from the Point of View of Classical Mean Field Theory

Aldo Bonasera

National Superconducting Cyclotron Laboratory
Michigan State University,
East Lansing, MI 48824-1321, U.S.A.

ABSTRACT

A simple classical force model, based on mean field dynamics, is applied to fusion phenomena and other processes in heavy ion collisions. We find reasonable agreement with trends in fusion cross section going to heavy nuclei, including the barrier to fusion at high Z^2/A. Collision times are calculated for a variety of reactions; recent evidence for non-equilibration of energy suggests that the equilibration time for energy is smaller than 300 fm/c and larger than 50 fm/c.

1. Introduction

Heavy ion collisions are a powerful tool to study the structure of nuclei. Many phenomena are found in heavy ion reactions depending on the many variables at the disposal of the experimenter. In the present work, we deal with low energy collisions, i.e. $E_{lab}<15$ MeV. In this energy regime, we can classify the reaction cross sections into three main types: quasi-elastic scattering, deep inelastic and fusion reactions.

Fusion occurs when the energy of the colliding nuclei is above the Coulomb barrier and for small impact parameters (neglecting sub-barrier fusion). This is not true for heavy systems. In that case, the Coulomb repulsion is too strong and an extra energy above the barrier is needed in order to keep the system in a coalesced state.

The second major category of reactions, the strongly damped collision, is characterized by a large amount of energy loss, but with the projectile and the target still maintaining something of their identity in the final state. Much information on the behavior of the nucleus can be obtained from this type of reaction. By analyzing typical examples of deep inelastic reactions, we will calculate the time the system takes to reach thermal equilibrium.

Quasi-elastic collisions occur in reactions in which the surfaces of the two ions have just been in grazing contact. Thus there is a small energy loss and a few nucleons are transferred from one nucleus to the other. This type of reaction is dominant at large impact parameters.

In this paper we will present a model that is suitable for describing collisions in which the nuclei come into close contact, and we will only discuss fusion and deep inelastic processes.

The microscopic basis of our model is TDHF theory that is, at present, the best justified model at low incident energy.[1,2] Unfortunately, the mean field theory is incomplete in several respects and due to computational difficulties its extension is not at all trivial.

We reduce TDHF to a classical form and we show that it is possible in this way to explain several different experimental results. The practical advantage of the classical model is that we need, for example, less than 5 sec of CPU time to calculate the trajectory for a fixed impact parameter, while using TDHF it takes 20 hrs. of CPU time for the same reaction.[3]

This work is organized as follows. In section 2 we present the formalism. Sections 3 and 4 are devoted to a comparison with experimental fusion cross section and the "extra-push" model respectively. Deep inelastic reactions are discussed in Section 5. Finally, we summarize our main results in section 6.

2. Equation of Motion

The classical equations of motion have been presented elsewhere.[1,2] We recall here the main results. A convenient way to reduce TDHF equation to a classical form is by taking its Wigner transform. In the limit $\hbar \to 0$, this gives the Vlasov equation:

$$\frac{df}{dt}(\vec{r},\vec{p},t) = \{h(\vec{r},\vec{p},t), f(\vec{r},\vec{p},t)\} \qquad (1)$$

where $h(\vec{r},\vec{p},t) = p^2/2m + W(\vec{r},\vec{p})$ is the Wigner transform of the self consistent HF hamiltonian and $f(\vec{r},\vec{p},t)$ is the phase-space distribution. The curly brackets indicate Poisson's brackets.

Classically the most important degrees of freedom are the conjugate variables $\vec{r}$ and $\vec{p}$ describing the relative motion of the two nuclei. We define these quantities as:

$$\begin{Bmatrix}\vec{r}\\ \vec{p}\end{Bmatrix} = \int_A d\vec{r}d\vec{p}\begin{Bmatrix}\vec{r}\\ \vec{p}\end{Bmatrix} f(\vec{r},\vec{p},t) - \int_B d\vec{r}d\vec{p}\begin{Bmatrix}\vec{r}\\ \vec{p}\end{Bmatrix} f(\vec{r},\vec{p},t) \tag{2}$$

where A and B refer to the two colliding nuclei. The Hamilton equations of motion of, say, nucleus A are found by taking the time derivative of Eq. (2) and using Eq. (1):

$$\frac{d}{dt}\begin{Bmatrix}\vec{r}_A\\ \vec{p}_A\end{Bmatrix} = \int_A d\vec{r}d\vec{p}\begin{Bmatrix}\vec{r}\\ \vec{p}\end{Bmatrix}\{h(\vec{r},\vec{p},t),f(\vec{r},\vec{p},t)\} \qquad \begin{pmatrix}3a\\ 3b\end{pmatrix}$$

Integration of Eq. (3a) by parts over $\vec{r}$ gives:

$$\frac{d}{dt}\vec{r}_A = \frac{\vec{p}_A}{m}$$

The jth component of Eq. (3b) reads:

$$\frac{d}{dt}P_{AJ} = \int_A d\vec{r}d\vec{p}\; p_j\left(\frac{p_i}{m}\partial_i f(\vec{r},\vec{p},t) + \partial_{pi}W(\vec{r},\vec{p})\partial_i f(\vec{r},\vec{p},t)\right.$$

$$\left. - \partial_i W(\vec{r},\vec{p})\,\partial_{pi}f(\vec{r},\vec{p},t)\right) + \text{Coulomb} \tag{4}$$

Integrating the second and third terms in parentheses by part over $\vec{p}$ and $\vec{r}$ gives:

$$\frac{d}{dt} P_{AJ} = \int_A d\vec{r}d\vec{p} \left(\frac{P_i P_j}{m} \partial_i f(\vec{r},\vec{p},t) + f(\vec{r},\vec{p},t)\delta_{ij}\partial_i W(\vec{r},\vec{p})\right) + \text{Coulomb} \qquad (5)$$

We define the momentum flux tensor as:

$$\tau_{ij} = \int_A d\vec{p} \frac{p_i p_j}{m} f(\vec{r},\vec{p},t)$$

Integrating over $\vec{p}$ and using Gauss theorem we finally get:

$$\frac{d}{dt} \vec{P}_A = \int_A d^2r \, \hat{n}\left[\tilde{\tau} + \tilde{1}\left(\frac{\rho \partial U}{\partial \rho} - U\right)\right] + \text{Coulomb} \qquad (6)$$

where we assume $U = \int W(\vec{r},\vec{p}) f(\vec{r},\vec{p},t) d\vec{p}$ is a local function of the density. Approximating the momentum flux tensor and the density with their value in nuclear matter we get:

$$\frac{d}{dt} \vec{P}_A = \pi r_N^2 \hat{n} \cdot \left[\tilde{\tau} + \tilde{1}\left(\frac{\rho \partial U}{\partial \rho} - U\right)\right]_{NM} + 2\pi\sigma r_N \hat{n} + \text{Coulomb} \qquad (7)$$

where r_N is the radius of the neck and σ is the surface energy. Equation (7) contains a delayed damping term given by the window formula.[1,2] The physical basis for the time delay is discussed in greater detail in the appendix. The monopole-monopole Coulomb force is a good approximation for light nuclei. For heavy systems we will use the parametrization of Ref. 8.

It was shown in Ref. 2 that a simple geometric parametrization for the neck radius is in good agreement with TDHF calculation. We further simplify and extend this prescription to asymmetric nuclei by assuming that in the approaching phase the radius of the neck is given by:

$$r_N = \alpha\sqrt{R_1+R_2-r}$$

and in the rebounding phase by:

$$r_N = r_{N_o} - \beta(r-r_o)$$

where r_{no} and r_o are respectively the neck radius and the relative distance at the closest approach. α=3.1 $fm^{1/2}$ and β=.60 are two parameters fitted to TDHF.[4]

Finally, we will assume that the two nuclei reseparate into two fragments in the rebounding phase if r_n<1 fm or a critical velocity for neck snap is exceeded.[1,2]

3. Fusion cross section

The formation of a compound nucleus requires first of all enough initial kinetic energy to overcome the Coulomb barrier. After touching, the surface tension opposes the Coulomb and centrifugal repulsion. Dissipation plays an important role. It is zero in the first stage after neck formation. In the second stage, the nucleon flux produces a strong pressure which suddenly reduces the relative velocity. This effect has clearly been shown in the reaction $^{40}Ca + ^{40}Ca$.[2] Moreover, this kind of dissipation prevents the two nuclei from reaching a spherical shape. Note that the sudden change between the first stage (superfluidity) and the second stage (superviscidity) can occur in the approaching phase as well as in the rebounding phase. This is very important and explains the occurrence of neck snap and the possibility of "cold fusion" (see below).

For light nuclei and low angular momentum the nuclear potential at the touching point is much stronger than the repulsive forces; so the nuclei will fuse once they touch. For high angular momentum, the centrifugal barrier will lead the composite system towards scission. The fusion cross section in this region is then mainly determined by the nuclear potential before the nuclei touch. For higher energies, we observe a rupture of the neck at zero impact parameter as well. This is an effect due to the time delay. At low energy, the superviscidity occurs in the approaching phase: the nuclei move then slowly and are trapped. But at higher energies the approaching phase is entirely superfluid: the relative velocity is very high and the occurrence of friction in the rebounding phase is not enough to avoid the overcoming of the critical velocity for neck snap. This effect is demonstrated in Fig. 1, where the time interval $\Delta T = tc - to$ is plotted versus energy. Here tc and to are the time at the turning and at the touching point respectively. The system is $^{40}Ca+^{40}Ca$ at zero impact parameter. We see that the time interval is larger than td up to 100 MeV and in this region we observe fusion. For larger energies the time delay is greater than ΔT, therefore the approaching phase is entirely superfluid and we get neck snap. For the system $^{16}O+^{16}O$, TDHF gives a window in the fusion cross section at energies ranging from 50 to 62 MeV in the laboratory, depending on the Skyrme interaction used. Such a prediction was tested experimentally at $E_{lab}=68$ MeV but the results are in disagreement with TDHF.[5] In Fig. 2 we plot the fusion cross section for $^{40}Ca+^{40}Ca$. Here two different sets of experimental data are plotted.[6,7] Our model is in better agreement with the data by Tomasi et al. and a repetition of the experiment by Barreto et al. confirms this set.[9] Unfortunately, there is only one experimental value at high energy and it is underestimated by our model. However if we add the

cross section for neck snap to the fusion cross section we get a value of 1057 mb. This estimate is much larger than the experimental value of 720 mb, thus supporting the existence of the low l-window. The conclusion is that there is still a great uncertainty both in theory and in experiments, suggesting the necessity to repeat these experiments at higher energies.

For very heavy systems the situation is quite different. The Coulomb repulsion is very strong, and the condition that the nuclei touch is not sufficient to get fusion. In this case the role of friction is changed as is clearly seen in Fig. 3 for the system $^{64}Ni+^{208}Pb$. At the energy where the nuclei touch, ΔT is just equal to the time delay, therefore the approaching phase is entirely superfluid while the rebounding is superviscid. This situation would, in this case, favor fusion; but the repulsion is too strong for a wide neck to be formed and the nuclei reseparate. For this reason, cold fusion as discussed by Swiatecki[10] cannot occur. The only possibility to get it would be for nuclei having a $(Z^2/A)eff.$ close to the threshold value. In general the fusion observed in this region is due to quantum fluctuations. It is very interesting to notice that in the first region the interaction time is very long, of the order of 700 fm/c. This might be a signature for fast fission.

A comparison of this model with experiments performed at GSI using a Pb beam, is shown in Fig. 4a,f.[11] There is a general good agreement with some discrepancies for the ^{48}Ca target. For impact parameters where fusion is predicted by experiments, we find an interaction time ranging from 500 to 1000 fm/c and this could explain the difference with experiments.

A comparison with experiments performed at MSU is shown in Fig. 5a,b.[12,13] In this case there is a systematic disagreement at higher energies. The interaction time is of the order of 300 fm/c and this

suggests that the system could have enough time to relax the initial mass asymmetry. Finally in Fig. 6a,e a comparison of the model with data for different systems is presented.[14-18]

4. Comparison with Extra Push Model

We demonstrated above how the necessity of an extra energy to get fusion arises quite naturally in our model. This is also a characteristic of Swiatecki's model and it is not surprising since both models are based on one-body dissipation. The main results of the extra push model are confirmed in our picture. A direct comparison between the two models is done in Figs. 7a,b for systems near the interesting region of superheavy elements. In the first graph the fusion and total reaction cross section is plotted for the system $^{209}Bi+^{54}Cr$.[10,19] Fusion for this system has been observed at the energies indicated by the arrows.[20] The Bass and proximity potentials give the same predictions for the total reaction cross section and therefore the slight discrepancies in the fusion region are due to other reasons. The same agreement is found for the reaction $^{248}Cm+^{48}Ca \rightarrow ^{296}X$. This reaction is very interesting because the compound nucleus has a neutron number close to the magic N=184 and it should be possible to detect experimentally.

5. Deep Inelastic Reactions

The very nature of the damping mechanism in heavy ion collision is still an open problem. The good agreement of our model with experimental fusion cross sections gives support to the concept of one-body dissipation. We expect two-body dissipation to become more and more important when the beam energy is increased.

The dominant process in the high energy region is the deep-inelastic reaction. Its main feature is the great energy loss, which suggests that the nuclei are strongly elongated in the exit channel. This occurs in our model in agreement also with TDHF calculation.[2] The large elongation of the two nuclei implies that they have a long interaction time. A large number of nucleons are exchanged between the two nuclei. The longer the system remains in contact, the more mass and charge is exchanged. The upper limit of this process is when the combined system fissions symmetrically. This case is very similar to fission following fusion but with a shorter interaction time (fast-fission). Therefore the angular distribution is not strictly symmetric in the C.M. system and can be distinguished experimentally.

We saw in the preceding sections that fast fission occurs in our model for heavy nuclei in the extra push energy region and for high angular momenta. These features have also been seen in TDHF.[21] We can think of fast fission as the border between fusion and deep-inelastic scattering.

At higher energies or angular momenta the interaction time becomes very short and pre-equilibrium processes occur. The main feature in this case is the emission of light particles in the early stage of the reaction. These particles are essentially neutrons and protons (Promptly Emitted Particles or Fermi jets), and for very high energy (>10 MeV/u), also α particles or even bigger nuclei.[22,23]

In Fig. 8, we plot the energy spectrum for the system $^{84}Kr+^{209}Bi$.[28] The peak at zero energy loss is due to quasielastic scattering. At higher energy there is a broad peak due to deep-inelastic scattering. Our model gives the correct position for the peaks but the magnitude of the cross section is overestimated. This is a limit of any classical model:

stochastic processes broaden all sharp structures. At medium energy losses the experimental data are underestimated. In this region of energy losses the nuclei are strongly elongated and there is a large mass transfer. Damping of mass asymmetry becomes important and should explain the discrepancy.[27]

Our model is in complete disagreement with experiments for the highest values of energy losses. At angular momenta close to the grazing value, the systems have a short interaction time and the neck snaps. This rapid process might result in more than two particles in the exit channel and this would explain the discrepancy.

Let us discuss now the results of a recent experiment on the $^{58}Ni+^{58}Ni$ and $^{58}Ni+^{197}Au$ systems at 15 MeV/u.[24] The purpose of this experiment was to check if thermal equilibrium is attained during the reaction. If this is true, we expect the available excitation energy to be shared in proportion to the masses of the projectile and the target.

For the system $^{58}Ni+^{197}Au$, the experimental angle-integrated charge distributions show a strong drift of the charge centroids away from symmetry. The light particle evaporation can be calculated under the hypothesis of thermal equilibrium. The values of the predicted charge centroids are larger than those observed. If the excitation energy is assumed to be shared equally between the two fragments, rather than according to the masses, the observed charge distributions are reasonably described. This conclusion is checked for the system $^{58}Ni+^{58}Ni$. Since the system is symmetric we expect an evaporation calculation to reproduce the experimental results. This is indeed the case.

An explanation of the nonthermal energy sharing is that at high bombarding energy, the system does not have enough time to reach thermal

equilibrium. In Fig. 9 we show the variation of the interaction time and the energy loss with impact parameter. The maximum value for the energy loss agrees with the experimental observation. The interaction time is very short, of the order of 10^{-22}sec. This implies a sudden rupture of the neck and the possibility of a three-body process in the exit channel.

The same considerations can be repeated for the system $^{56}Fe+^{165}Ho$ at 8.5 MeV/u. At this lower energy, the centroids of the charge and neutron distributions are well described by assuming a smooth transition from the limit of equal sharing of the dissipated energy occurring at small energy loss, to the limit of equal temperature at large energy loss.[24] In Fig. 10 we plot the interaction time and energy loss versus impact parameter. For b less than 4.6 fm we get fusion. The fusion cross section is 665 mb which agrees nicely with experimental data. At higher impact parameters, our model gives a very long interaction time, of the order of 10^{-21} sec. In this case the system has enough time to reach thermal equilibrium. For the highest values of impact parameters, the interaction time is equal to that for the system $^{58}Ni+^{197}Au$, resulting in a pre-equilibrium process. Therefore it is not surprising that the best description of the data is given by a smooth transition as described above.

Our model suggests that the time the system takes to reach equilibrium is surely larger than 50 fm/c and smaller than 300 fm/c. Bertsch has determined the local equilibrium time by considering the equilibration of a quadrupole deformation of the Fermi sphere within the Fermi-gas approximation.[25] His numerical result is in good agreement with the above estimate.

6. Conclusions

We have set up a classical model for heavy ion collisions based on the known bulk dynamics of mean field theory. With our parameterization of the forces arising in mean field theory, it is possible to reproduce results of TDHF as well as experimental data on fusion and deep inelastic reactions. The most important part of the force is associated with particle transfer. This force is not dissipative in the early stage of the reaction. Thus there are two distinct phases during the reaction: superfluid and superviscous. Conversely, our potential interaction includes a surface force which has a dissipative part, due to the exit shape being different from the entry shape.

Calculations using the classical equations of motions are very easy to perform, thus it could also be possible to extend the model. For example, an extension could regard fast particle emissions in the early stages of the reaction or an explicit treatment of the mass drift in order to reach a better understanding of the phenomenon of fast fission.

Acknowledgments

I am grateful to Prof. G.F. Bertsch for very useful discussions during this investigation and for critically reading the manuscript.

Appendix

The basic assumption in the derivation of the window formula is that at low excitation energy the mean free path of the nucleons is larger than the nuclear diameter. Damping arises only when the nucleons hit the surface of the nucleus. We expect the friction is delayed to allow the nucleons to cross the entire nucleus and hit the surface opposite to the small window formed between the two colliding nuclei. A similar mechanism acts for giant resonances. In this case we can imagine a nucleon, excited by the surface oscillation, travelling freely in the nuclear medium and interacting with the mean field, after a time

$$t_d = 2R/\bar{v} \tag{A1}$$

where R is the radius of the nucleus and $\bar{v} = \frac{3}{4} v_f$ is the mean velocity in a Fermi gas. This is a characteristic time for the system, and represents the rate of change of the collective energy of the nucleus due to the interaction with different degrees of freedom. According to the uncertainty principle the minimum energy spread of the resonance, Γ, is given by:

$$\Gamma = \hbar/t_d = 17\ A^{-1/3}\ \text{MeV} \tag{A2}$$

where we used standard values for R and the Fermi velocity.

This functional dependence was suggested in Ref. 26 as an experimental fit to the empirical data. The wall formula predicts the same A dependence but with a larger coefficient. This simple estimate works quite well for monopole and quadrupole widths, as shown in Figs. A1 and A2. For higher multipolarities, in particular the giant octupole, the experimental values

are larger than predicted by Eq. (A2). However our main purpose is to show that dissipation via a time delay parameter is reasonable and in agreement with dissipation of very collective motion. Thus for the time delay we will use the value given by Eq. (A1).

References

1. G.F. Bertsch, MSU preprint (1982).
2. A. Bonasera, G.F. Bertsch, and E.N. El-Sayed, Phys. Lett. 141B (1984) 9.
3. H. Stöcker, private communication, and H. Stöcker et al., Z. Phys. A306 (1982) 235.
4. A. Dhar and B. Nilsson, Phys. Lett. 77B (1978) 50.
5. A. Lazzarini et al., Phys. Rev. C24 (1981) 329.
6. H. Doubre et al., Phys. Lett. 73B (1978) 135.
7. E. Tomasi et al., Nucl. Phys. A373 (1982) 341.
8. J.E. Poling et al., Phys. Rev. C13 (1979) 659.
9. J. Barreto et al., Phys. Rev. C27 (1983) 1335.
10. W.J. Swiatecki, Nucl. Phys. A376 (1982) 275.
11. R. Bock et al., Nucl. Phys. A388 (1982) 334.
12. M.B. Tsang et al., MSU preprint, Feb. 1983.
13. M.B. Tsang et al., MSU preprint (1983).
14. J.R. Birkelund et al., Phys. Rev. C27 (1983) 882.
15. H.C. Britt et al., Phys. Rev. C13 (1976) 1483.
16. H. Gauvin et al., Phys. Lett. 58B (1975) 163.
17. B. Tamain et al., Nucl. Phys. A252 (1975) 187.
18. C. Cabot et al., J. Physique 41 (1980), suppl. C.10, 234.
19. S. Bjørnholm et al., Nucl. Phys. A391 (1982) 471.
20. G. Münzenberg et al., Z. Phys. A300 (1981) 107.
21. K. Davies et al., Nuclear Physics with Heavy Ions, 1983, p. 57.
22. M. Bühler et al., Proc. Workshop on Nuclear Dynamics III, Colorado 1984, p. 105.
23. J.P. Bondorf et al., Nucl. Phys. A333 (1980) 285.

24. T.C. Awes et al., Phys. Rev. Lett. 52B (1984) 251.

25. G.F. Bertsch, Z. Phys. A289 (1978) 103.

26. A. Van Der Wolde, Giant Multipole Resonances, Vol. I, p. 65 (Harwood Academic Publishers), and references therein.

27. J. Randrup and W.J. Swiatecki, LBL preprint, Jan. 1984 (submitted to Nucl. Phys.

28. J.R. Huizenga, et al., Phys. Rev. Lett. 37 (1976) 885.

Figure Captions

Fig. 1 - Time interval ΔT (see text) versus energy in the C.M. system for the system $^{40}Ca+^{40}Ca$. At E_{CM}=100 MeV, ΔT is equal to the time delay t_D=38 fm/c.

Fig. 2 - Fusion cross section versus energy for the system $^{40}Ca+^{40}Ca$. Data points are from Refs. 6 (x's) and 7 (dots).

Fig. 3 - Same as Fig. 1 for the system $^{208}Pb + ^{64}Ni$. The time delay t_D is explicitly indicated in the figure.

Fig. 4a-f - Fusion cross section versus Energy in the C.M. for different systems. Data points are from Ref. 11.

Fig. 5a,b - Same as Figs. 4a-f, the experimental data were taken from Refs. 12 and 13.

Fig. 6a-d - Comparison of the classical model with experimental data on fusion, Refs. 14-18.

Fig. 7a,b - Reaction (full line) and fusion cross section (dashed line) calculated using the present model as compared to the results of the "extra push" model (dots and squares respectively), Refs. 10 and 19.

Fig. 8 - The Energy loss spectrum for the system $^{84}Kr + ^{209}Bi$ at E_{LAB}=712 MeV. The experimental curve is from Ref. 28.

Fig. 9 - Interaction time and energy loss versus impact parameter for the system $^{58}Ni + ^{197}Au$.

Fig. 10 - Same as Fig. 9 for the system $^{56}Fe + ^{165}Ho$. Note that for b less than 4.6 fusion occurs.

Fig. A1 - Experimental isoscalar monopole width versus mass number compared with Eq. (A2), full line. Experimental data are from Ref. 26.

Fig. A2 - Same as Fig. A1 for the quadrupole case.

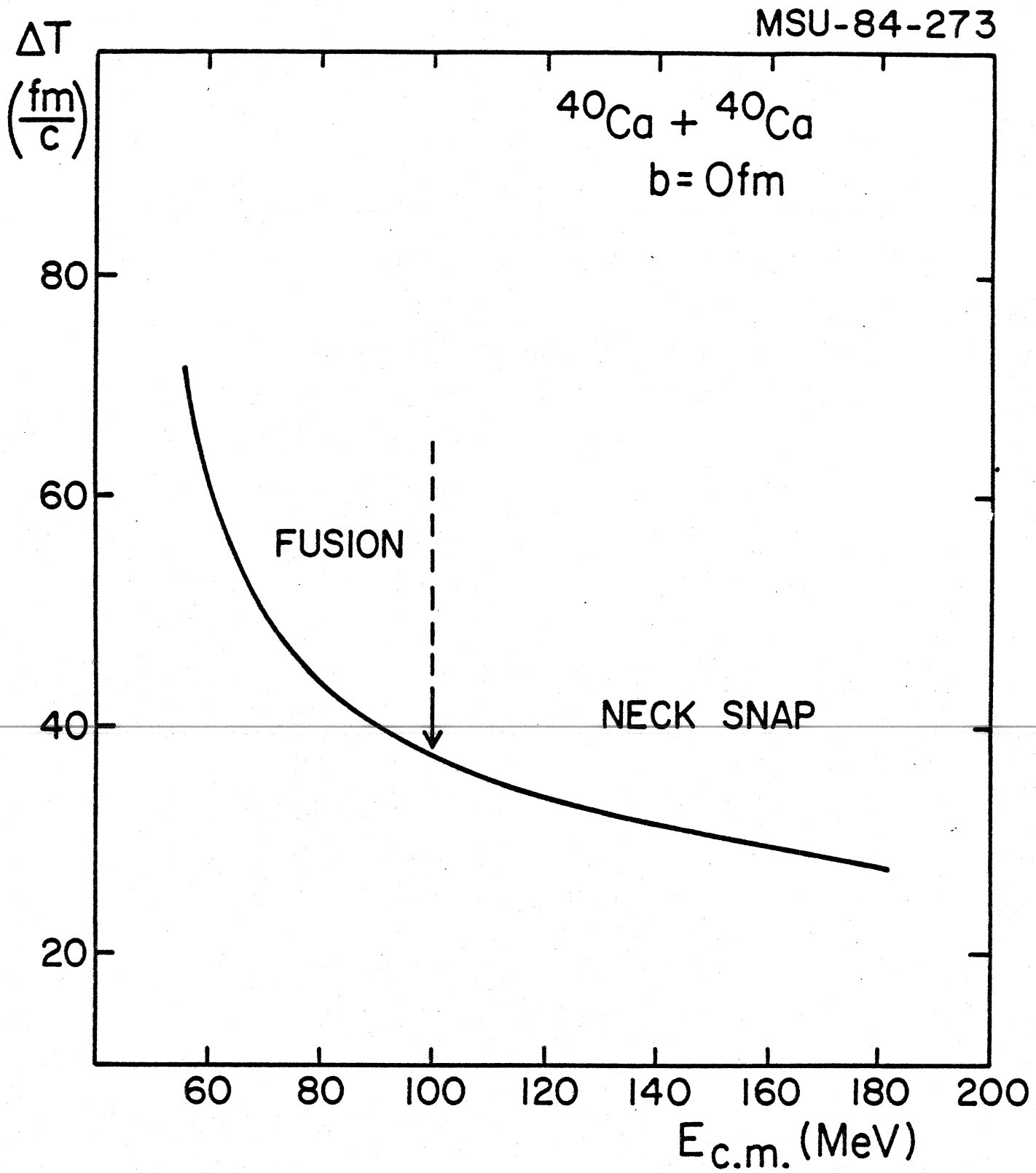
MSU-84-273
ΔT
(fm/c)
40Ca + 40Ca
b = 0fm
80
60
40
20
FUSION
NECK SNAP
60
80
100
120
140
160
180
200
Ec.m. (MeV)

FIGURE 1

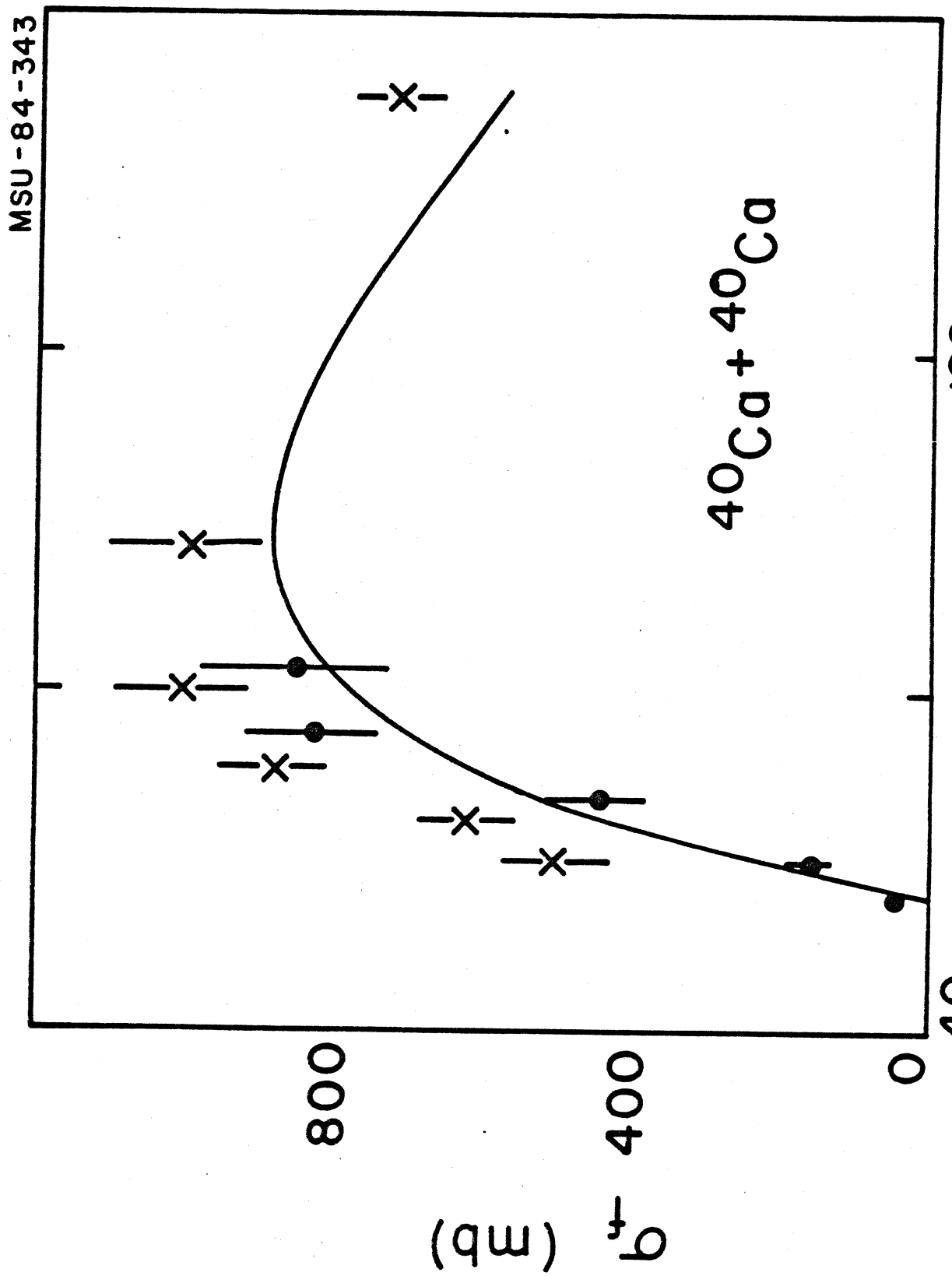

FIGURE 2

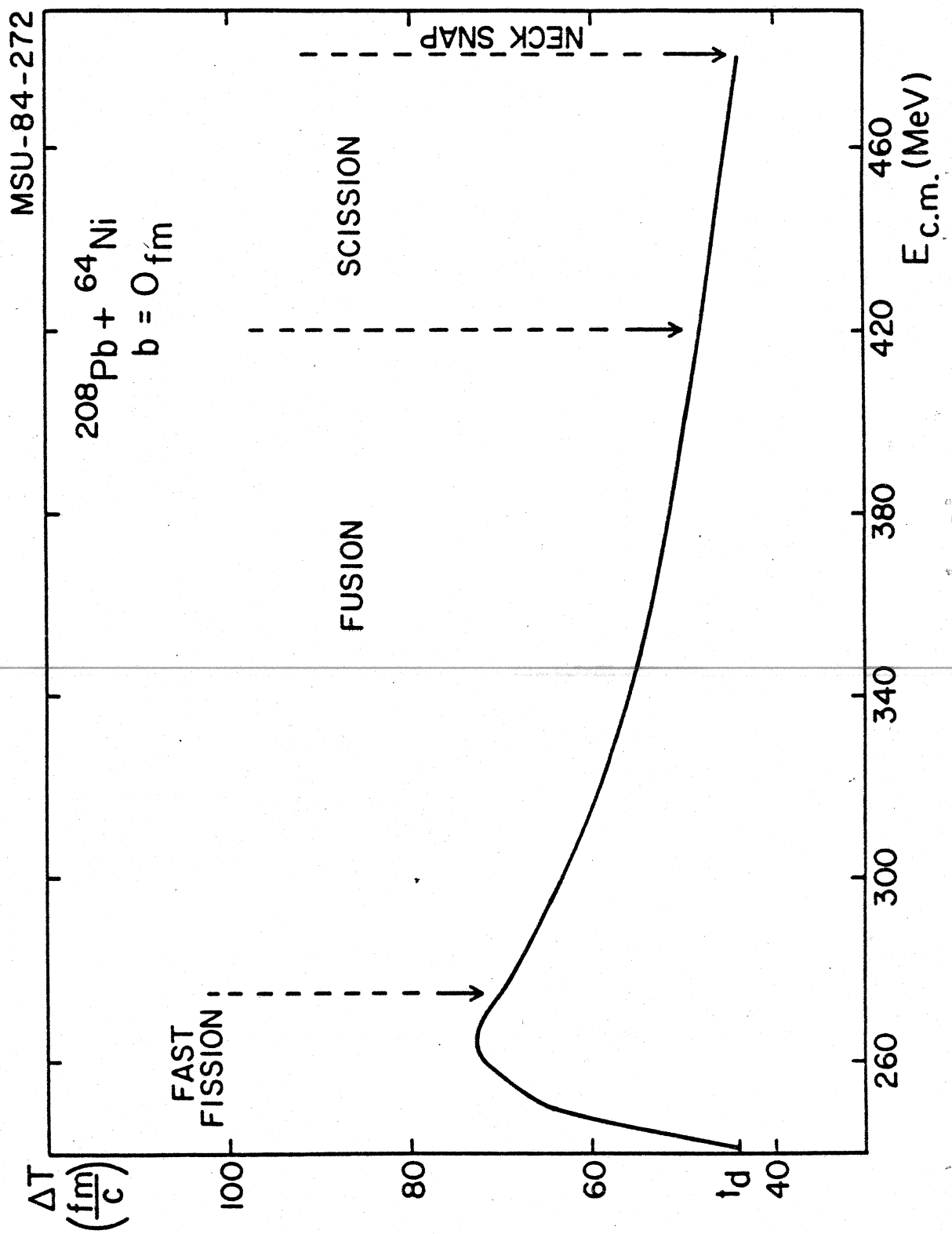
MSU-84-272
$^{208}Pb + ^{64}Ni$
b = 0 fm
NECK SNAP
SCISSION
FUSION
FAST FISSION
$\Delta T \left(\frac{fm}{c}\right)$
100
80
60
40
t_d
260
300
340
380
420
460
$E_{c.m.}$ (MeV)

FIGURE 3

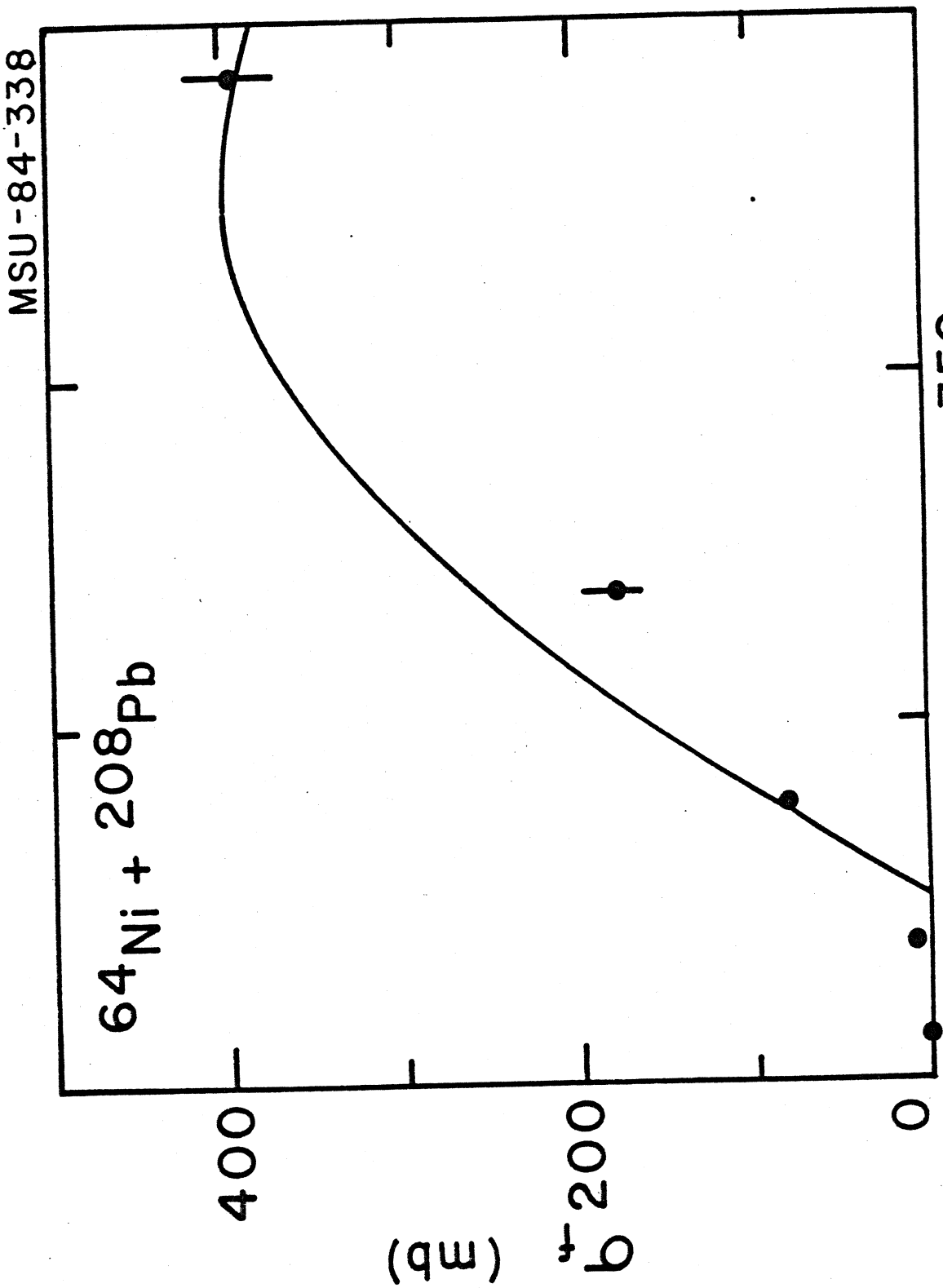

FIGURE 4a

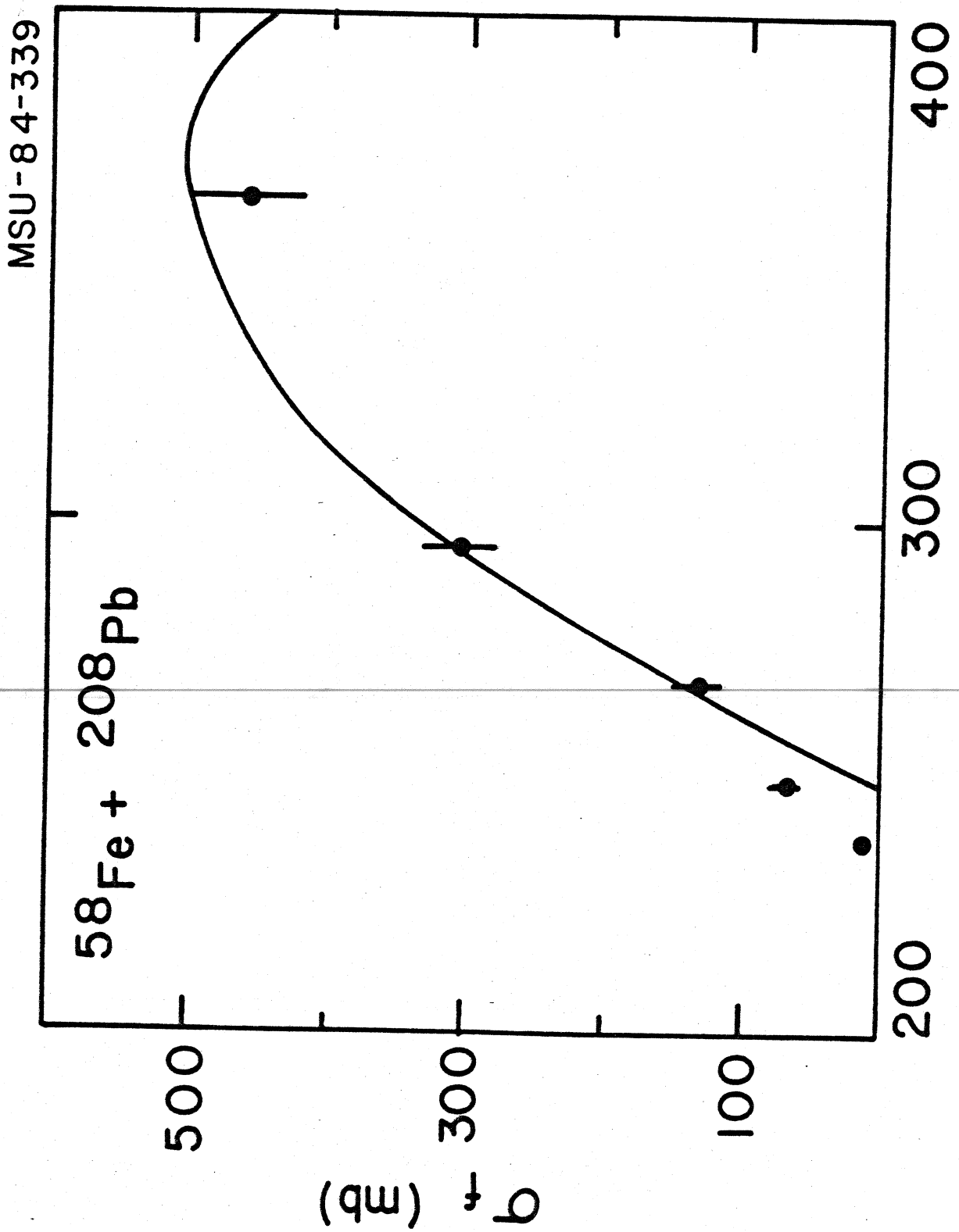

FIGURE 4b

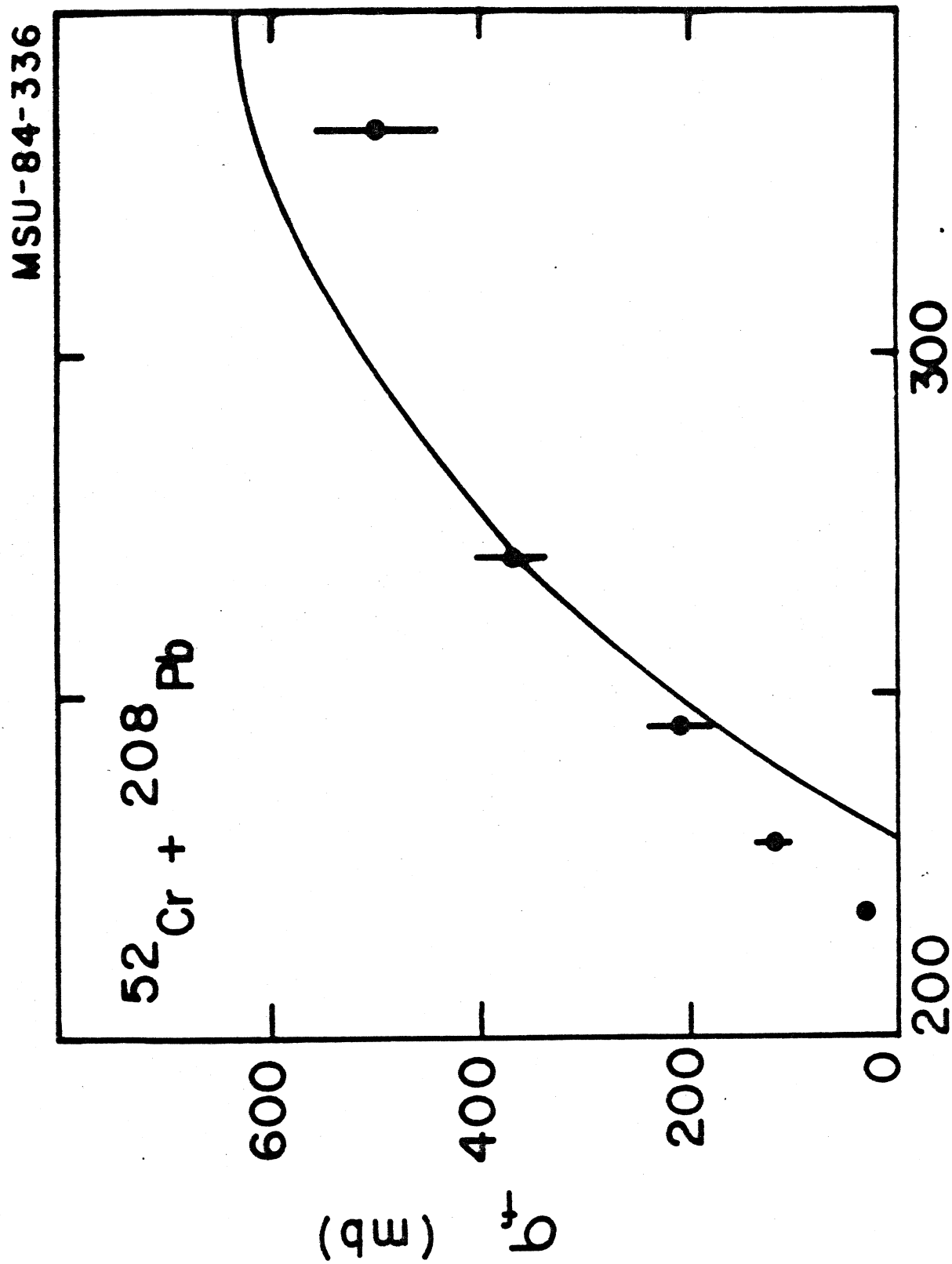

FIGURE 4c

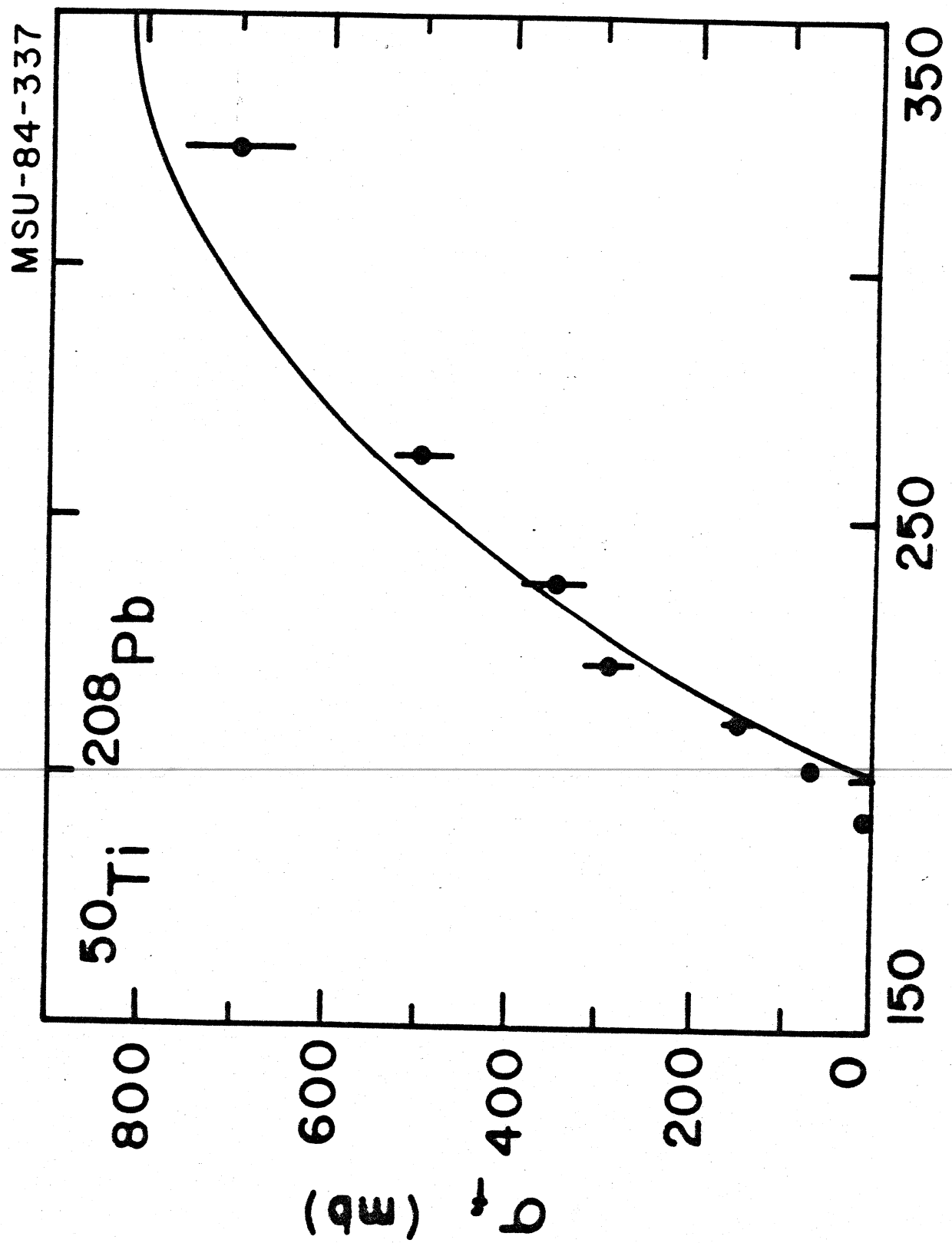
MSU-84-337
^{50}Ti ^{208}Pb
σ_f (mb)
800
600
400
200
0
150
250
350
$E_{c.m.}$ (MeV)

FIGU. 4d

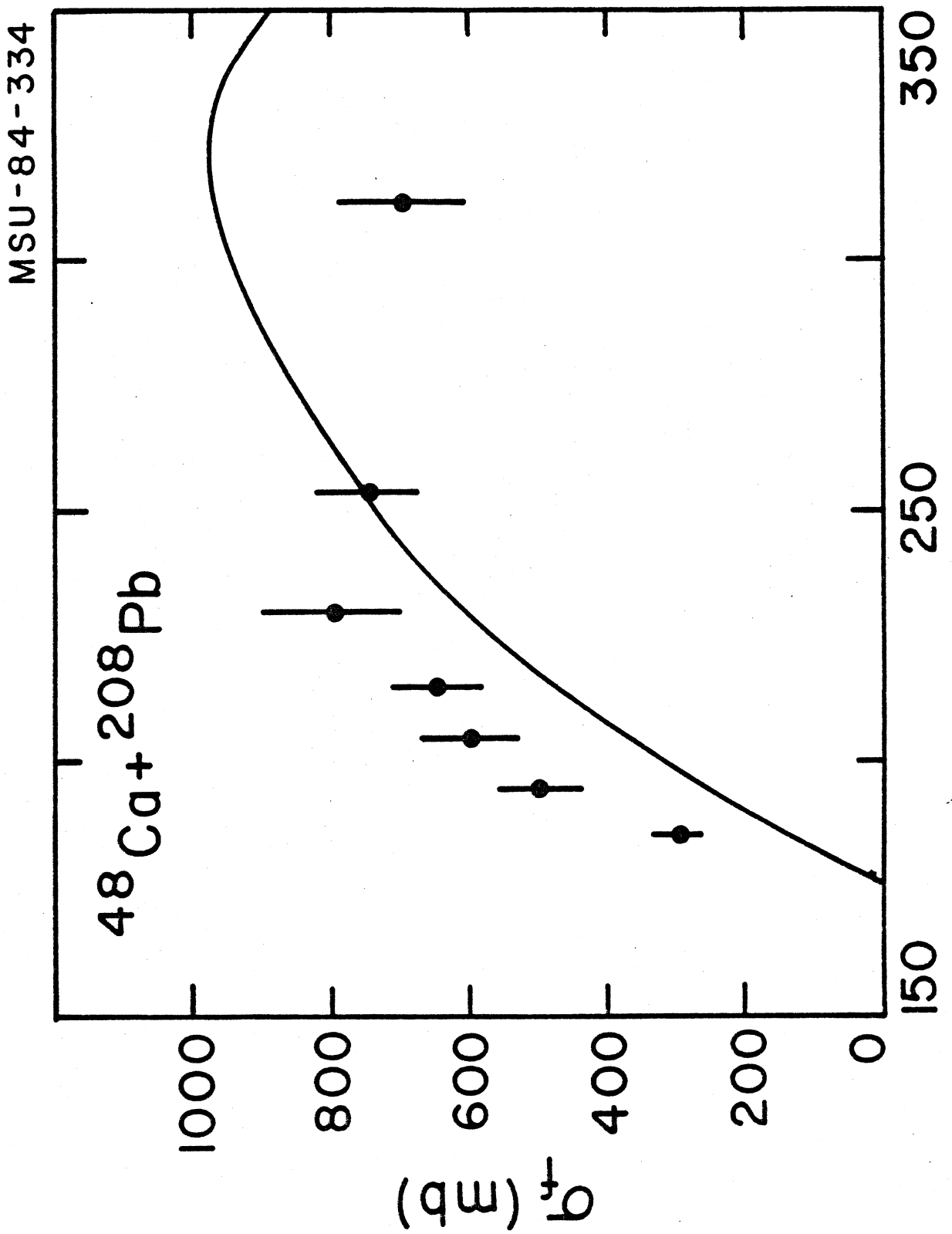
MSU-84-334
$^{48}Ca + ^{208}Pb$
σ_f (mb)
0
200
400
600
800
1000
150
250
350
$E_{c.m.}$ (MeV)

FIGURE 4e

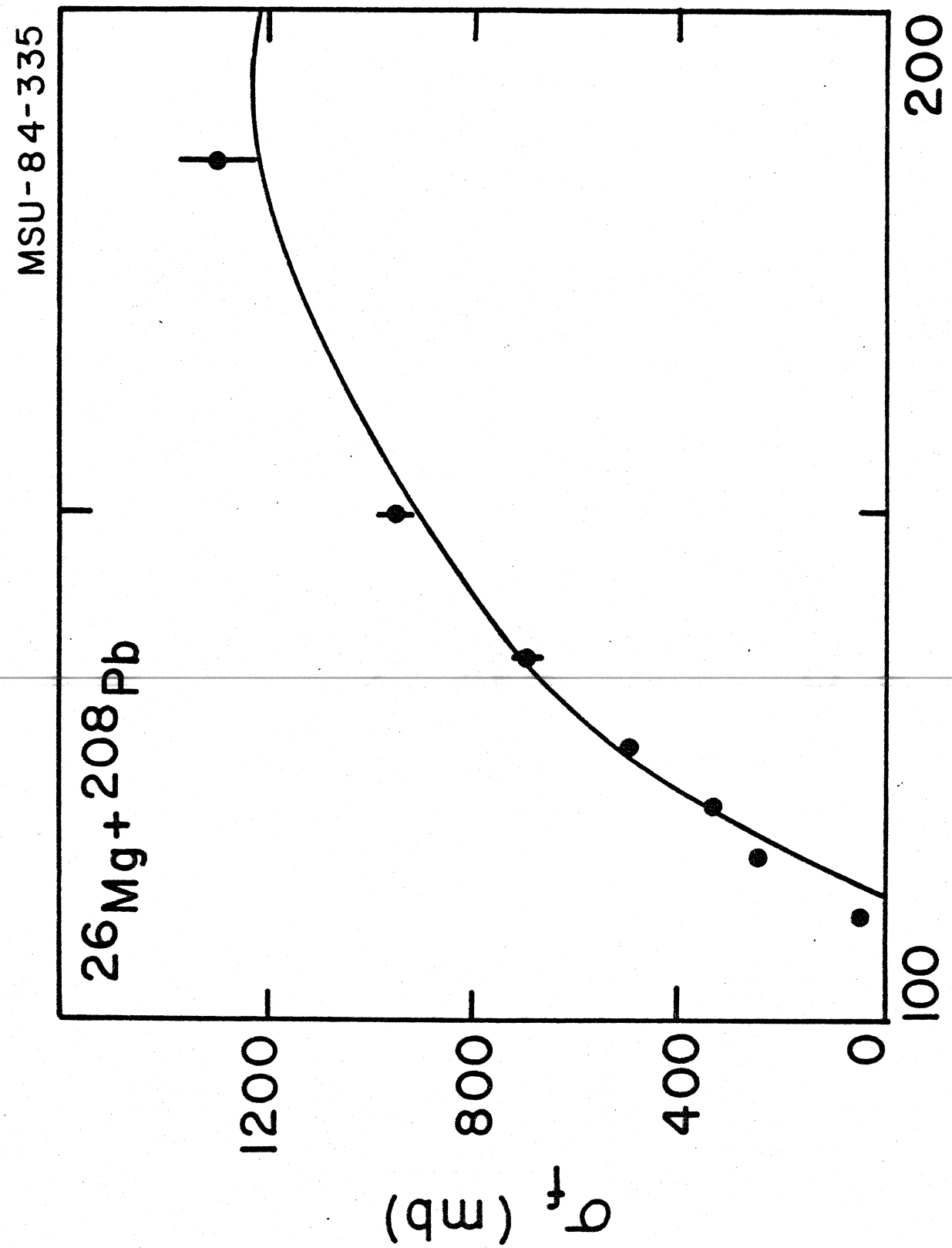

FIGURE 4f

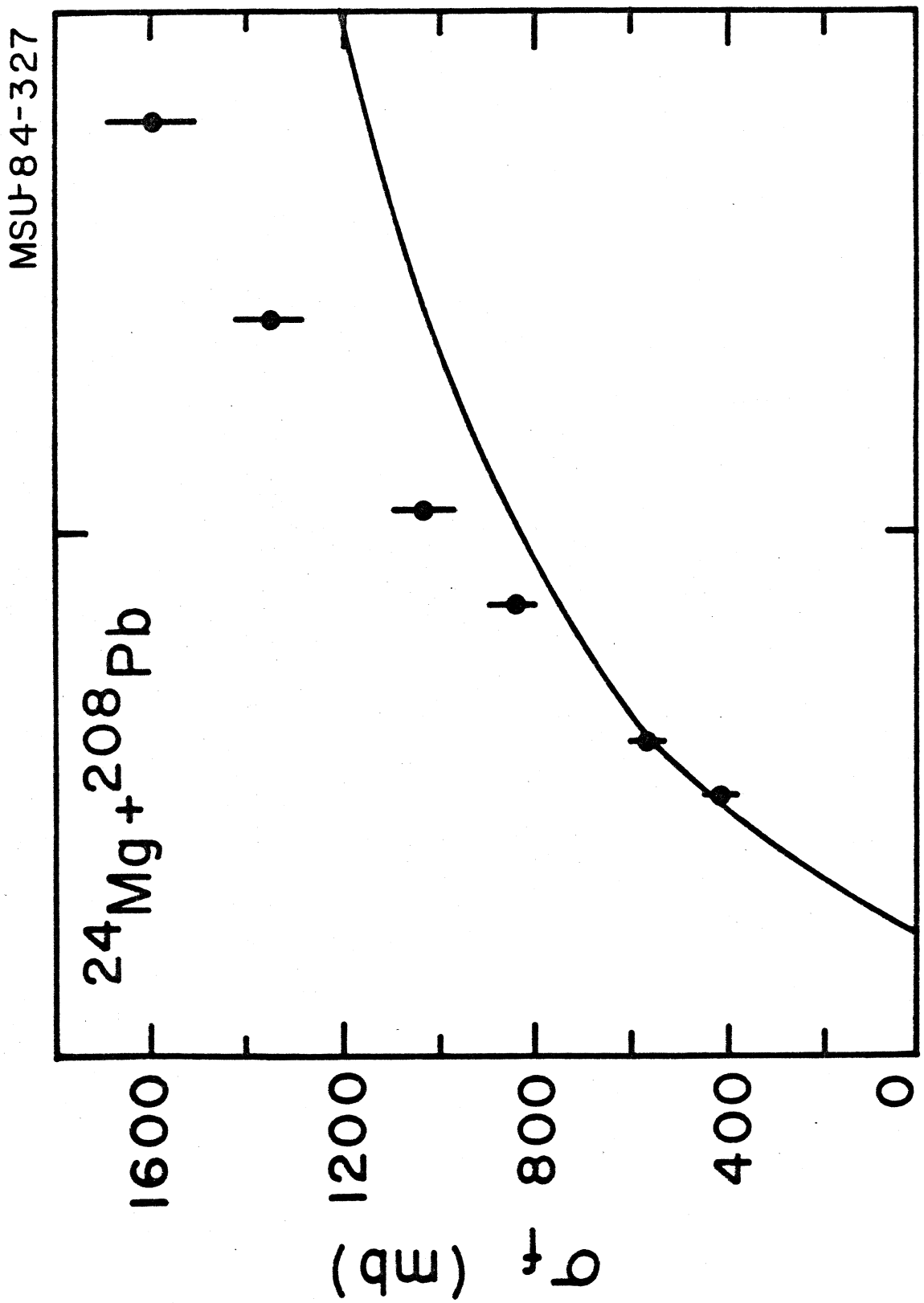
MSU-84-327
$^{24}Mg + ^{208}Pb$
σ_f (mb)
1600
1200
800
400
0
100
200
$E_{c.m.}$ (MeV)

FIGURE 5a

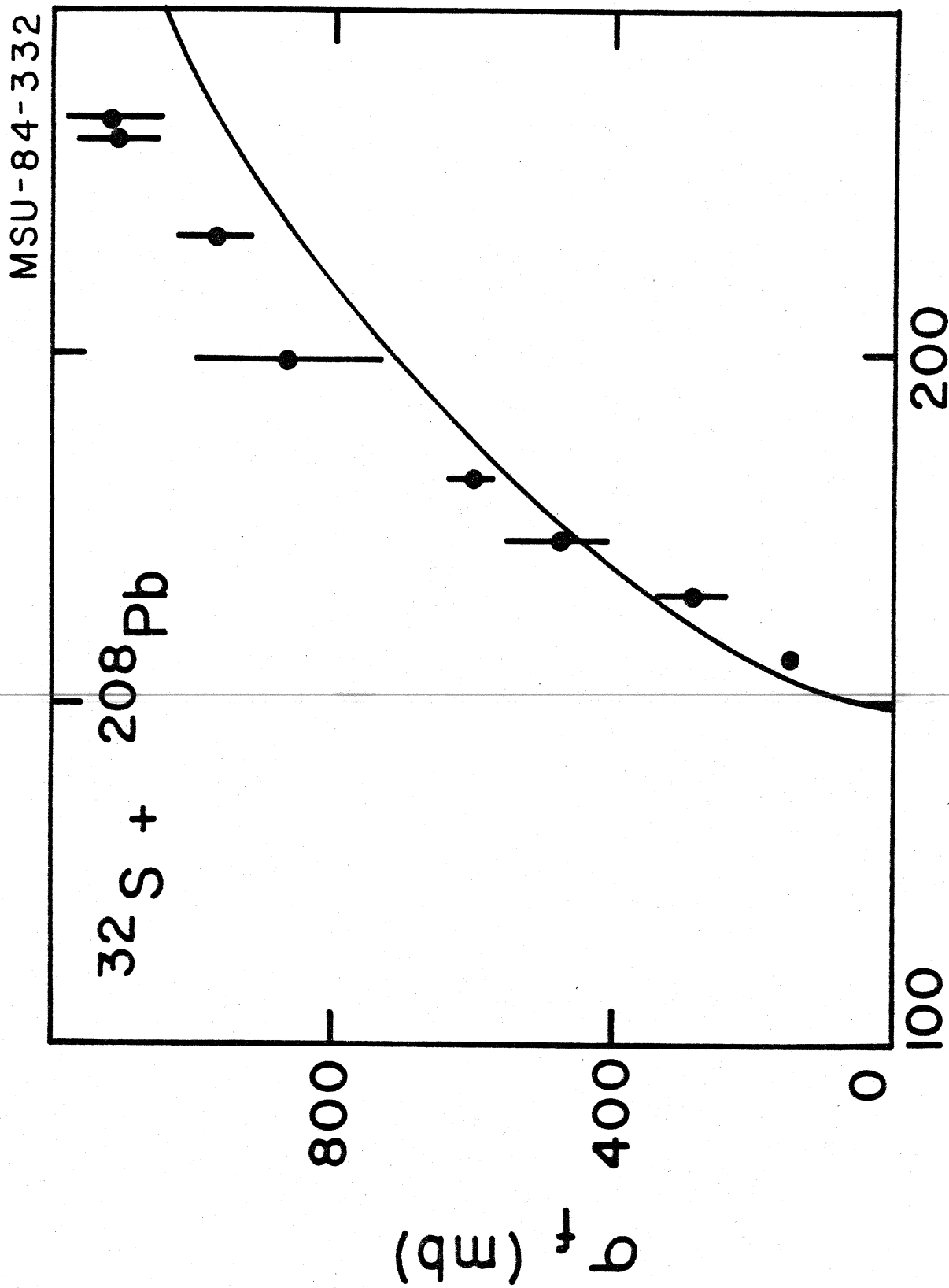

FIG. 5b

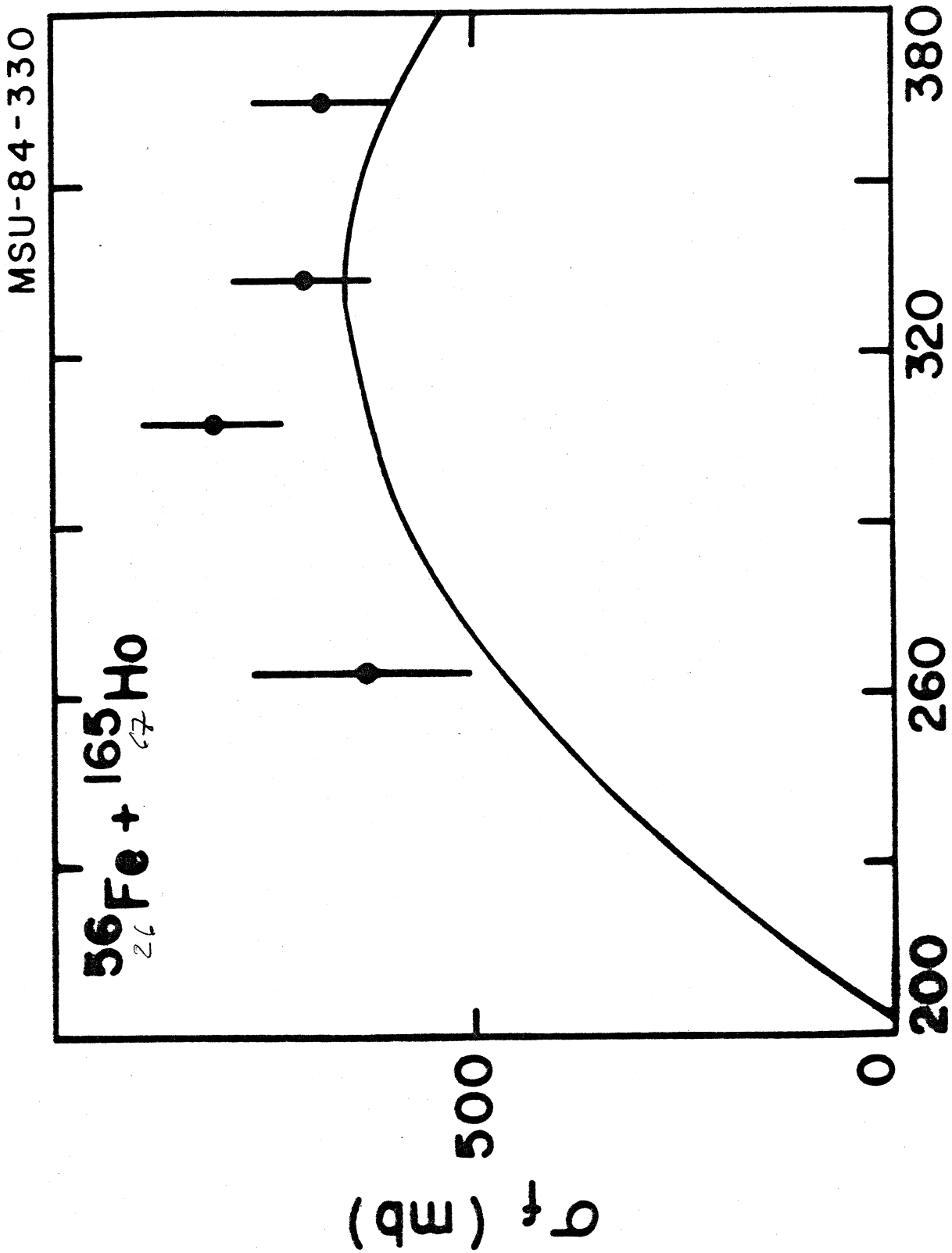
MSU-84-330
$^{56}_{27}Fe + ^{165}_{67}Ho$
σ_f (mb)
500
0
200
260
320
380
$E_{c.m.}$ (MeV)

FIGURE 6a

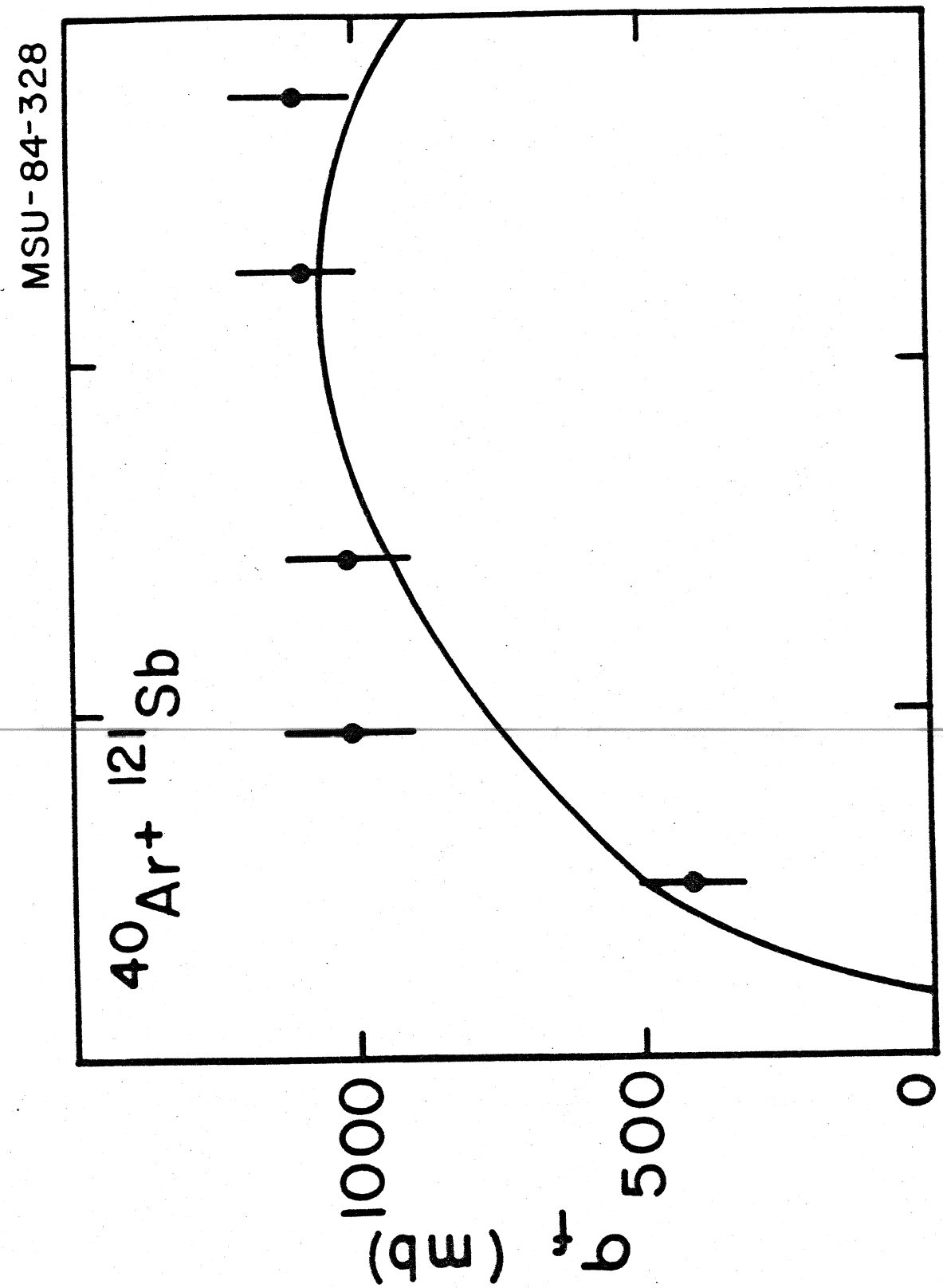

FIG. 6b

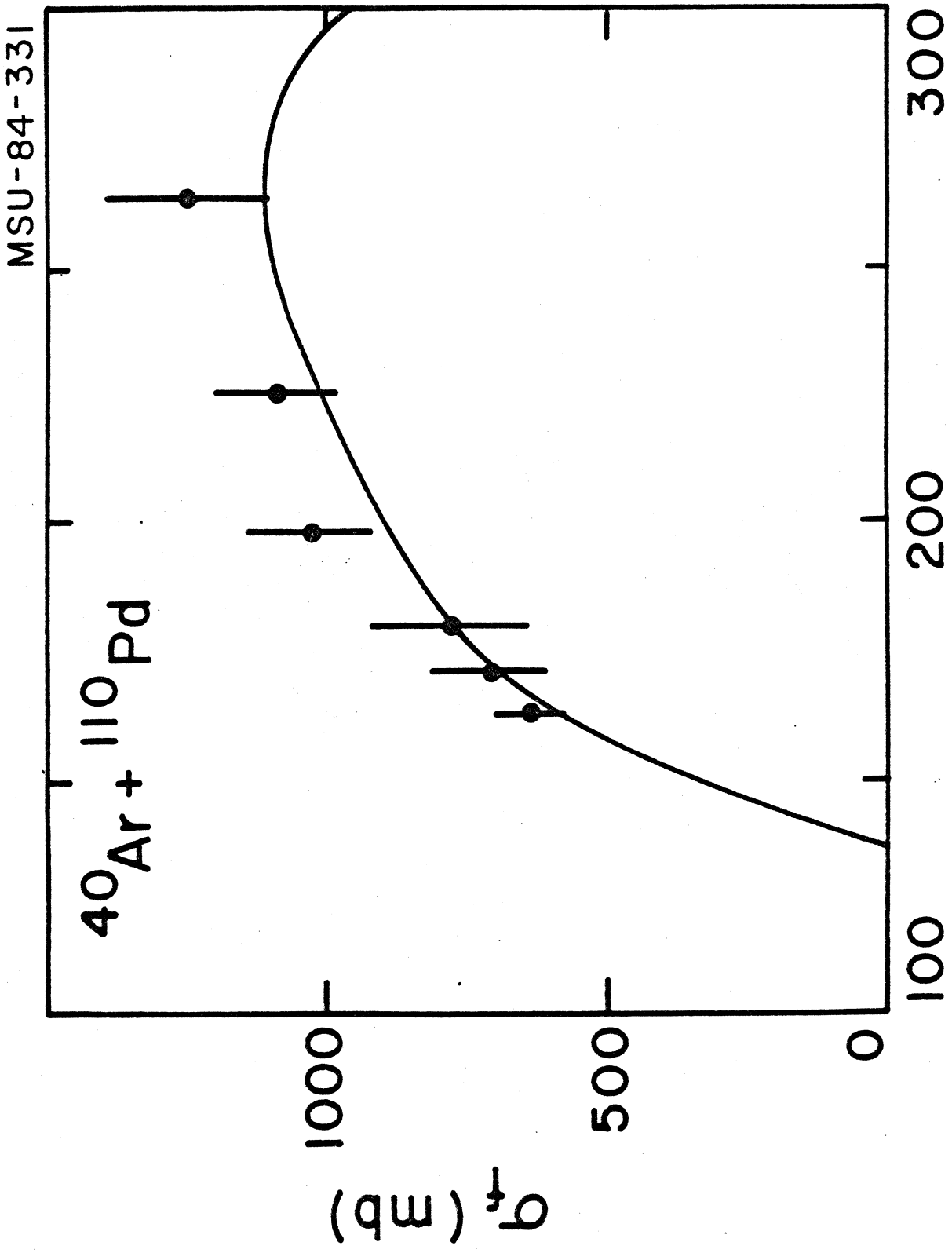

FIGURE 6c

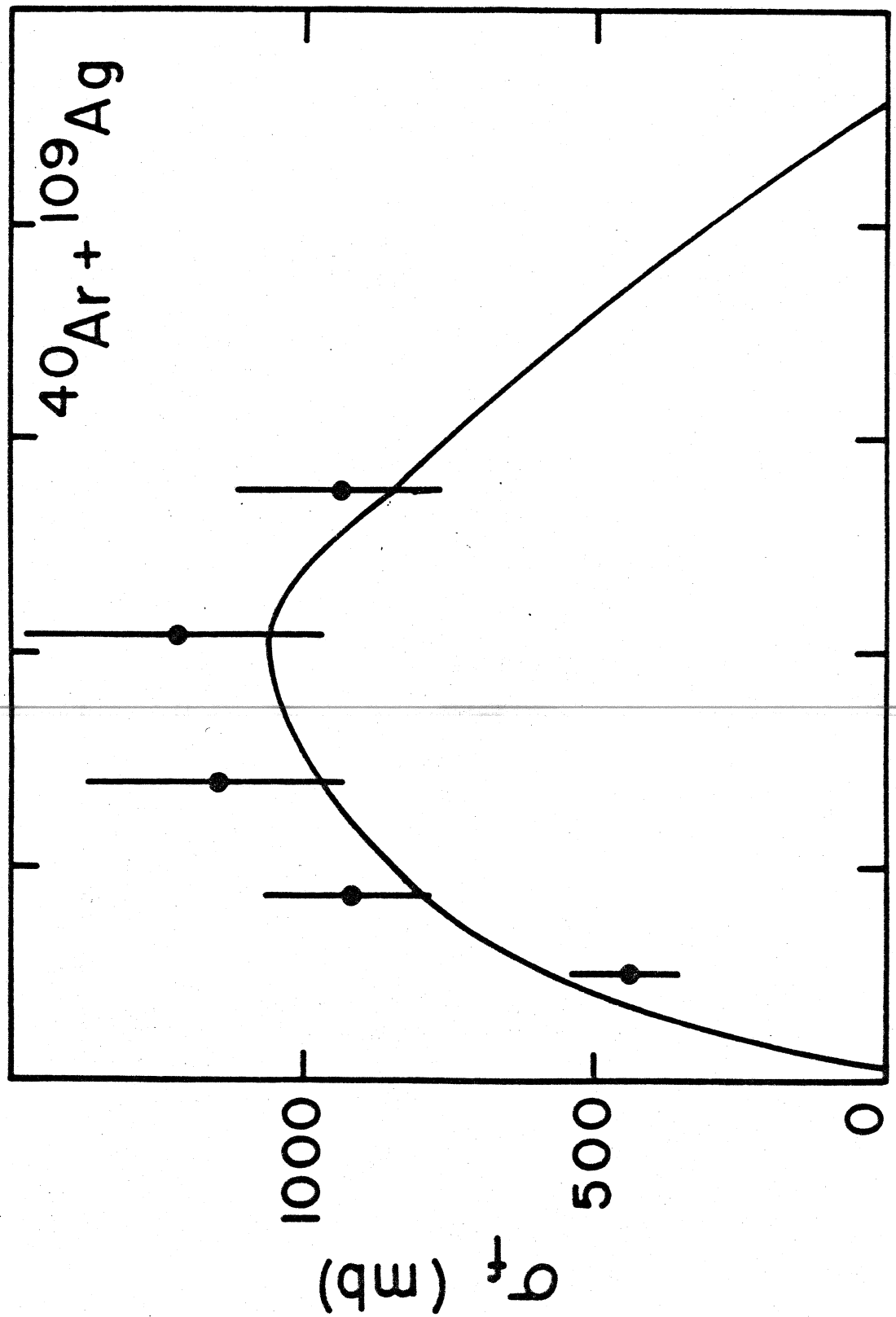

FIGURE 6d

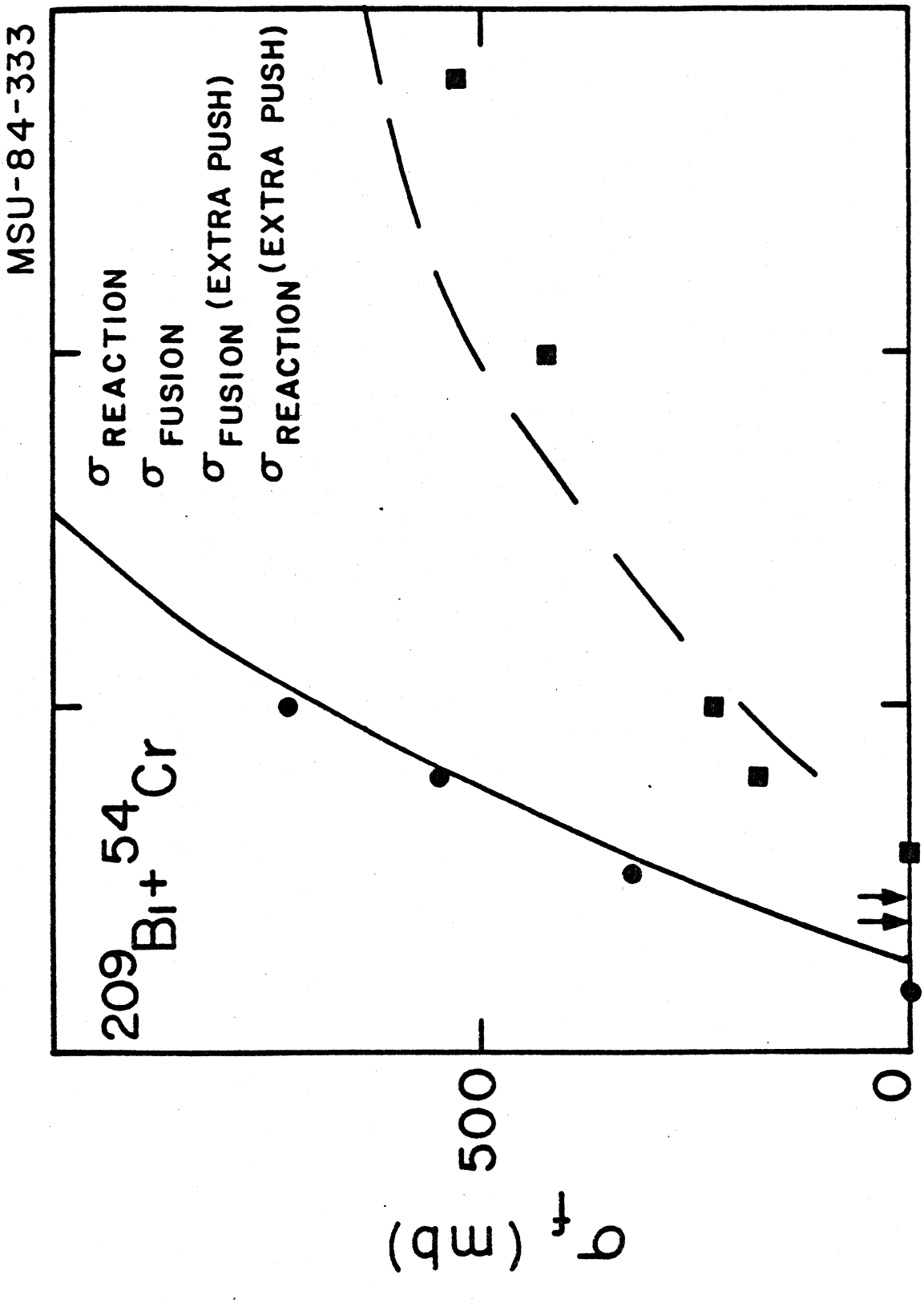
MSU-84-333
$\sigma_{REACTION}$
σ_{FUSION}
$\sigma_{FUSION\ (EXTRA\ PUSH)}$
$\sigma_{REACTION\ (EXTRA\ PUSH)}$
$^{209}Bi + ^{54}Cr$
q_f (mb)
500
0
200
300
$E_{c.m.}$(MeV)

FIGURE 7a

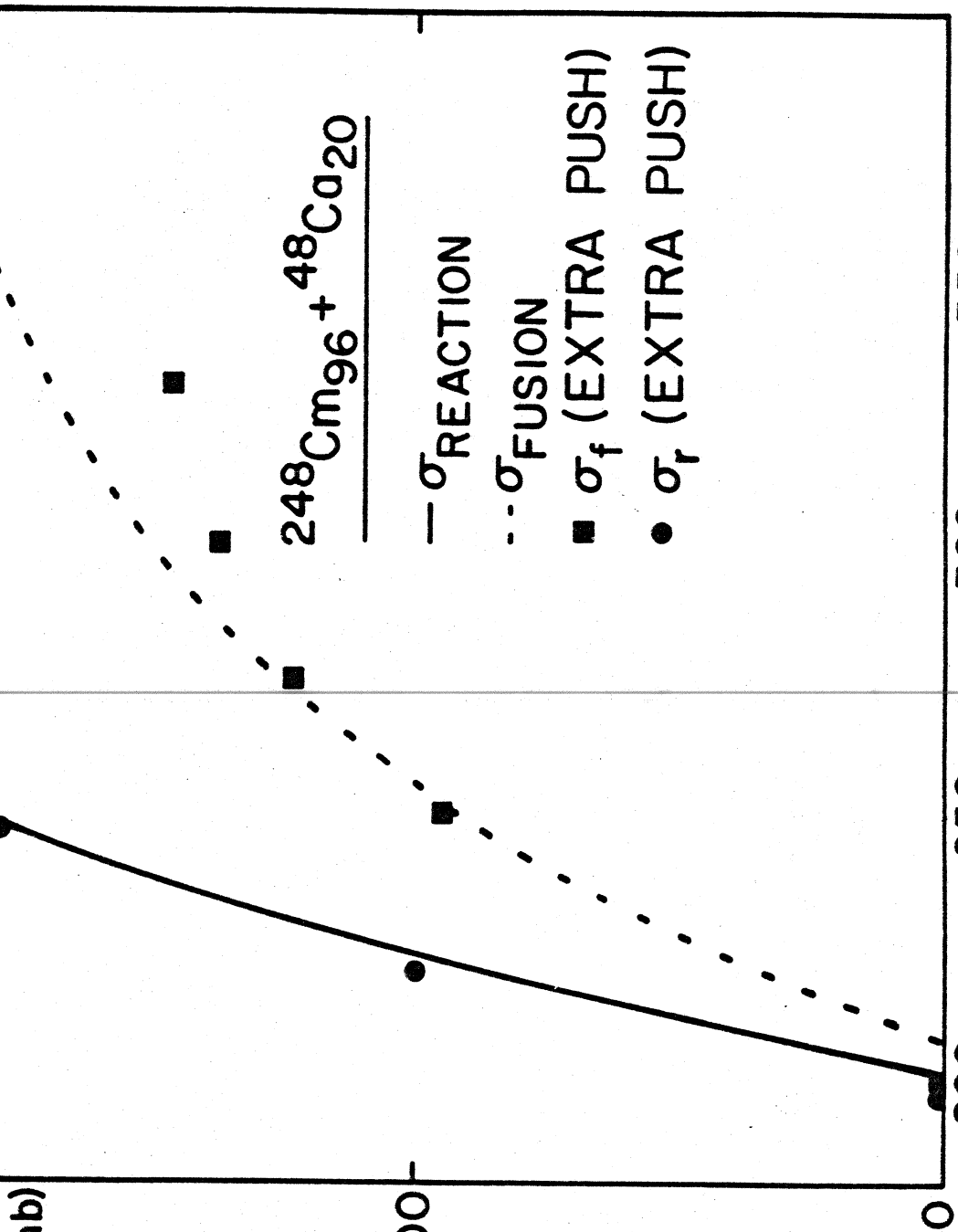
MSU-84-269
$^{248}Cm_{96} + ^{48}Ca_{20}$
$-\sigma_{REACTION}$
$--\sigma_{FUSION}$
$\blacksquare\ \sigma_f$ (EXTRA PUSH)
$\bullet\ \sigma_r$ (EXTRA PUSH)
σ_f(mb)
0
500
200
250
300
350
$E_{c.m.}$(MeV)

FIG. 7b

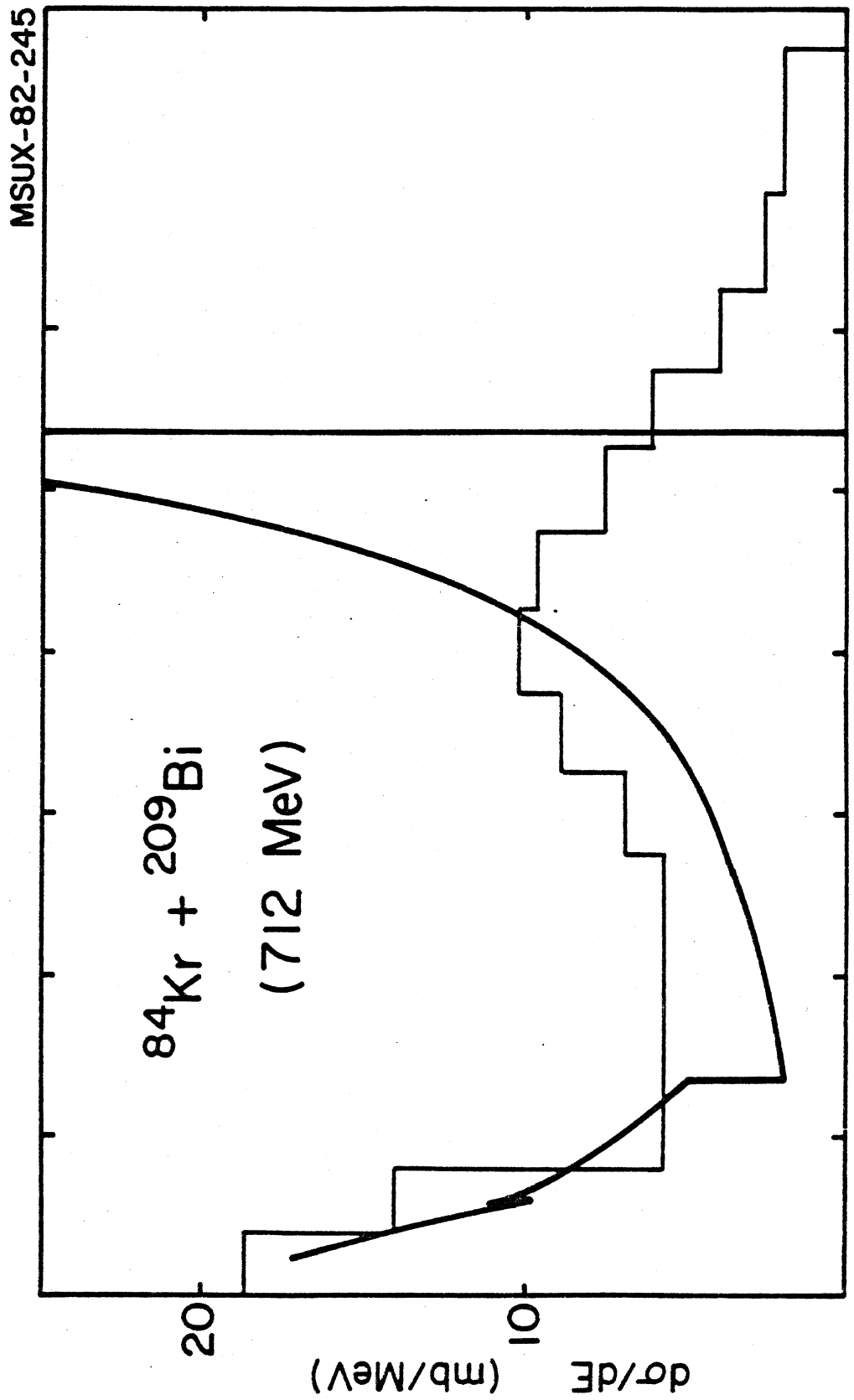
MSUX-82-245
$^{84}Kr + ^{209}Bi$
(712 MeV)
dσ/dE (mb/MeV)
20
10
100
200
300
TOTAL KINETIC ENERGY LOSS (MeV)

FIGURE 8

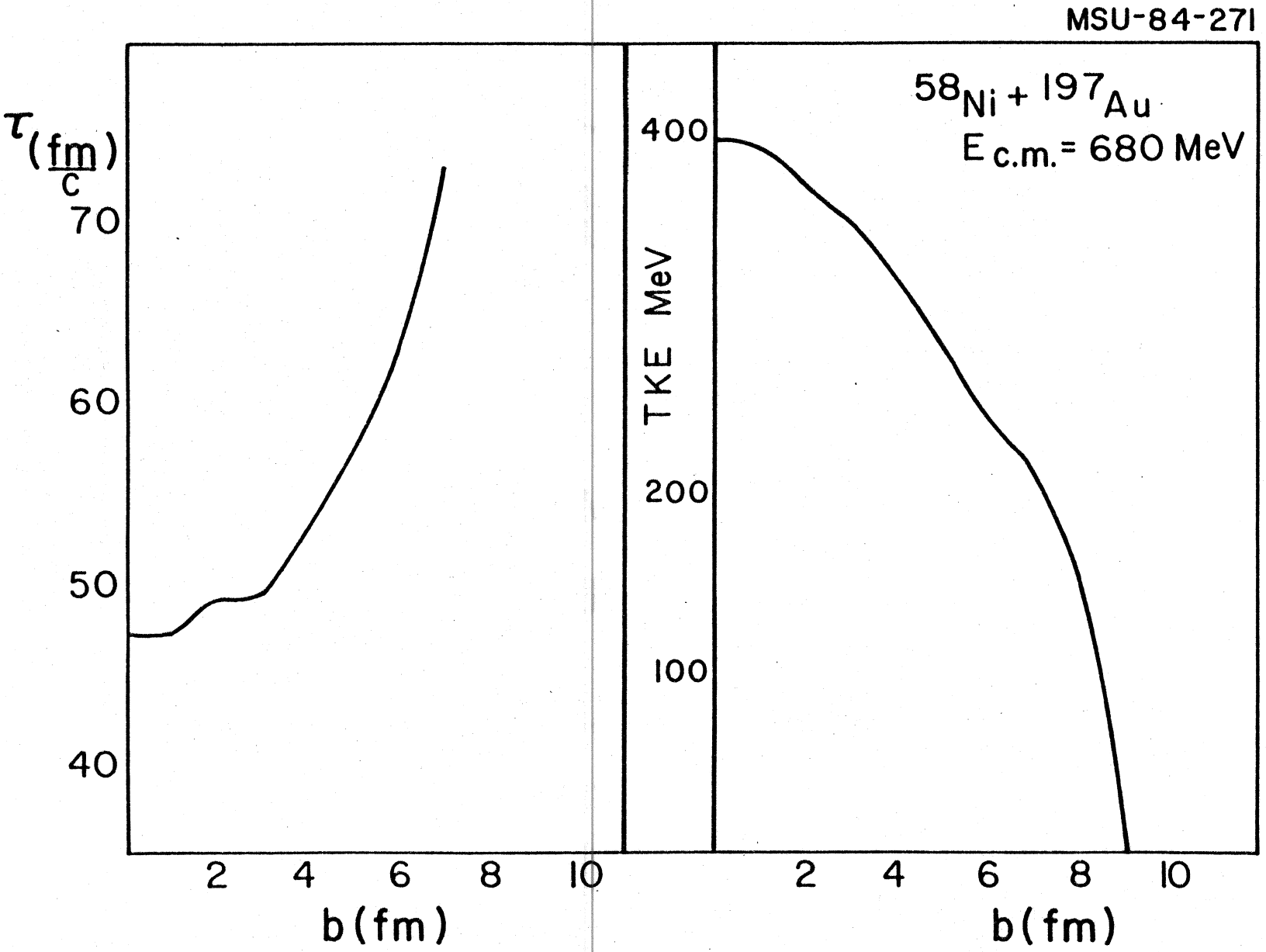
MSU-84-271
$^{58}Ni + ^{197}Au$
E c.m. = 680 MeV
$\tau_{(\frac{fm}{c})}$
70
60
50
40
TKE MeV
400
200
100
2
4
6
8
10
b(fm)
2
4
6
8
10
b(fm)

FIGU 9

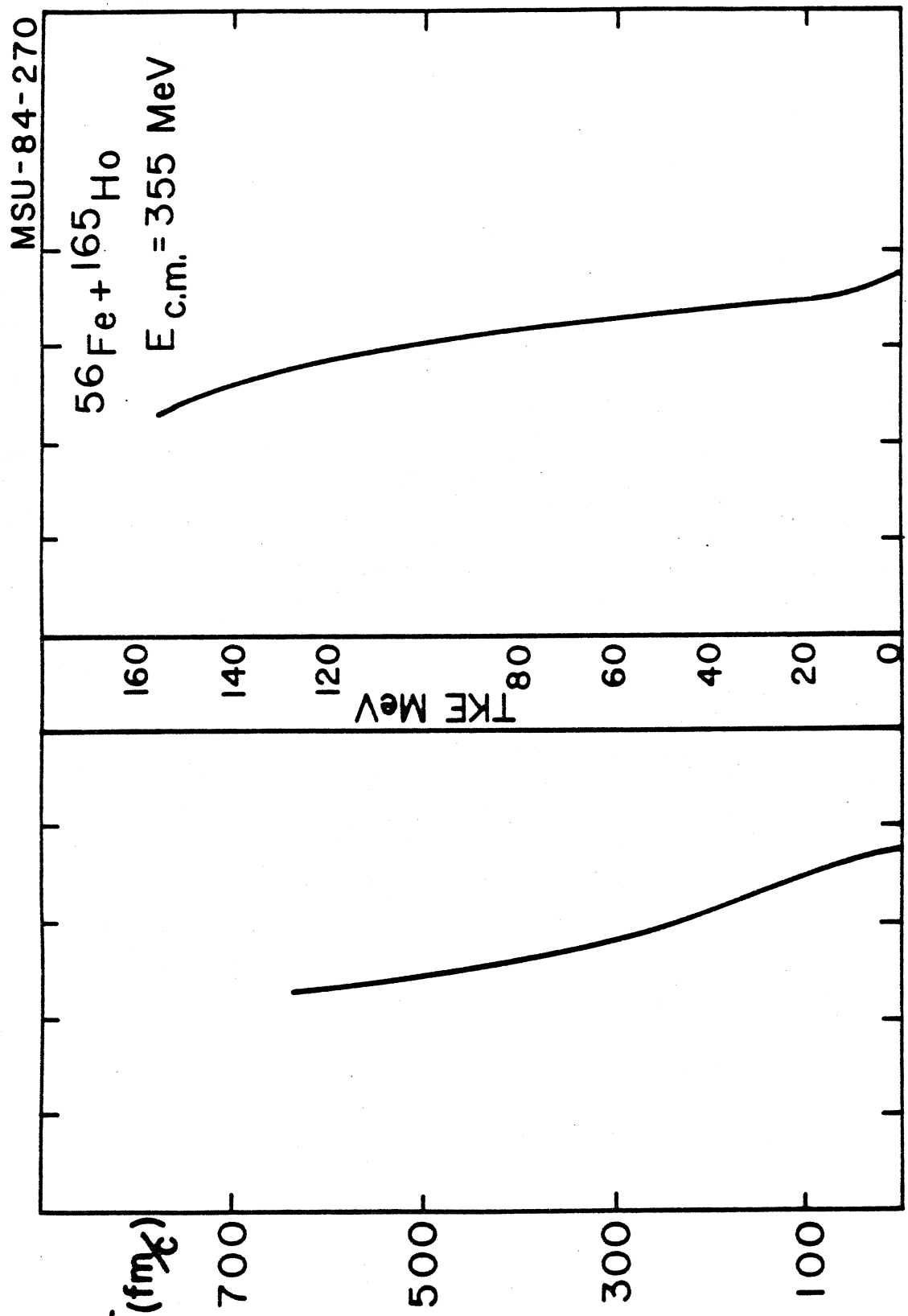
MSU-84-270
$^{56}Fe + ^{165}Ho$
$E_{c.m.} = 355$ MeV
TKE MeV
160
140
120
80
60
40
20
0
2
4
6
8
b(fm)
$\tau_{(fm/c)}$
700
500
300
100
2
4
6
8
b(fm)

FIGURE 10

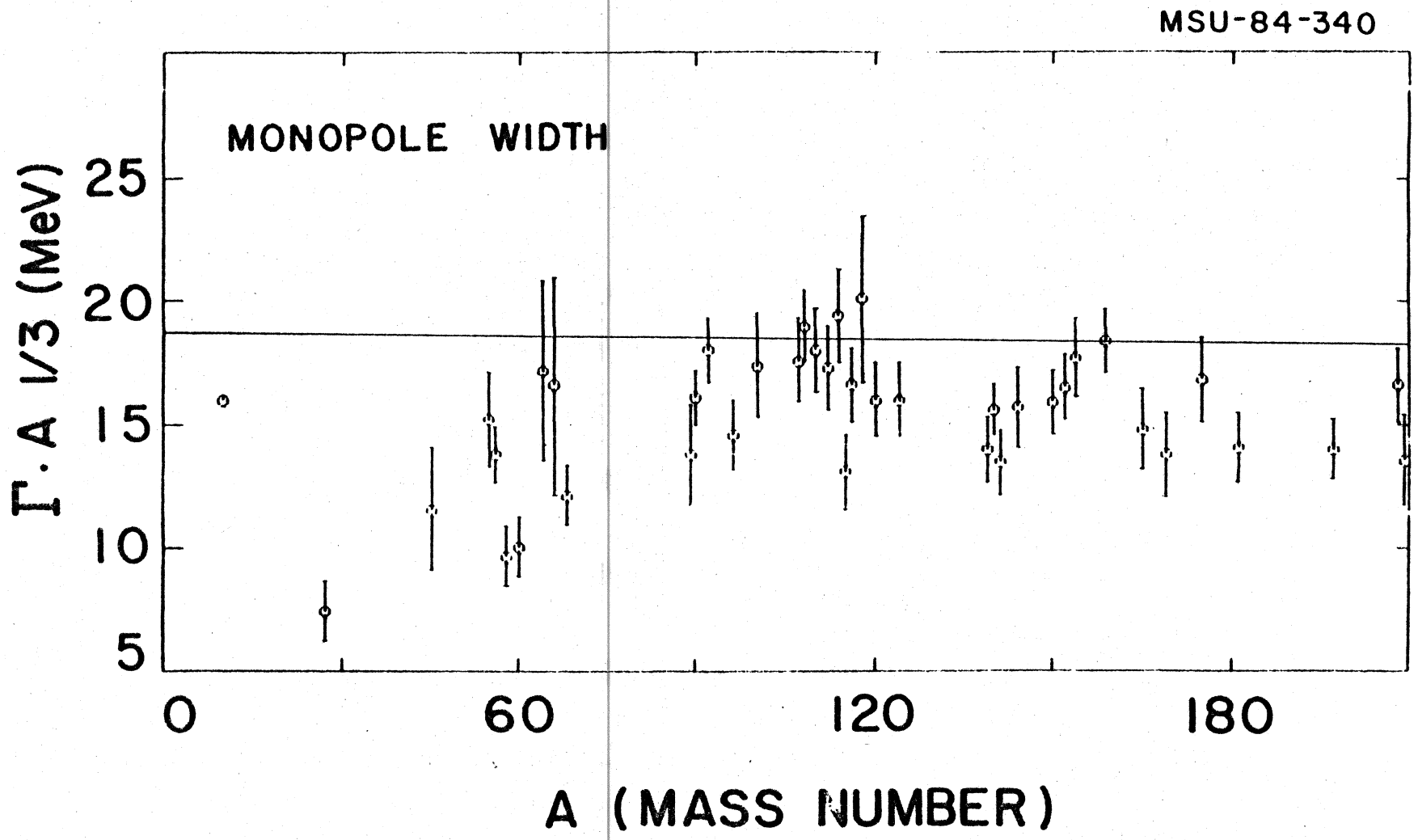
MSU-84-340
MONOPOLE WIDTH
Γ·A 1/3 (MeV)
25
20
15
10
5
0
60
120
180
A (MASS NUMBER)

FIGURE 1

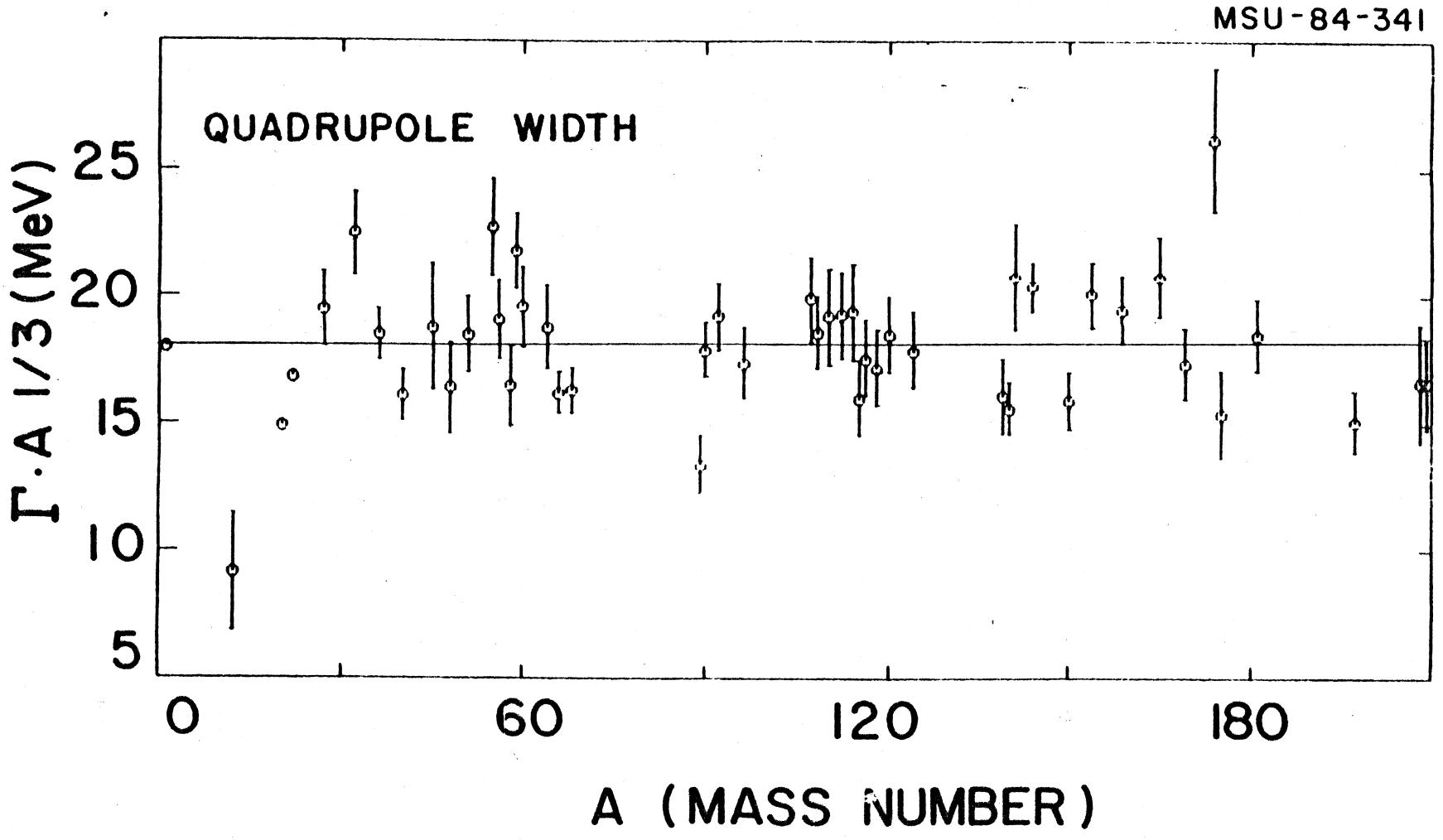
MSU-84-341
QUADRUPOLE WIDTH
Γ·A 1/3 (MeV)
25
20
15
10
5
0
60
120
180
A (MASS NUMBER)

FIGURE A2